SPECIAL ISSUE

Plant, Cell &
Environment

WILEY

Phytochelatin and coumarin enrichment in root exudates of arsenic-treated white lupin

Adrien Frémont[1] | Eszter Sas[1] | Mathieu Sarrazin[2] | Emmanuel Gonzalez[3,4] |
Jacques Brisson[1] | Frédéric Emmanuel Pitre[1,5] |
Nicholas James Beresford Brereton[1]

[1]University of Montreal—Institut de Recherche en Biologie Végétale (IRBV), Montreal, Quebec, Canada

[2]Collège de Maisonneuve—CÉPROCQ, Montreal, Quebec, Canada

[3]Canadian Centre for Computational Genomics (C3G)—Department of Human Genetics, McGill University, Montreal, Quebec, Canada

[4]Microbiome Research Platform—McGill Interdisciplinary Initiative in Infection and Immunity (MI4), Genome Centre, McGill University, Montreal, Quebec, Canada

[5]Montreal Botanical Garden, Montreal, Quebec, Canada

Correspondence
Nicholas James Beresford Brereton, University of Montreal—Institut de Recherche en Biologie Végétale (IRBV), 4101 Sherbrooke Street E, Montreal, QC H1X 2B2, Canada.
Email: nicholas.brereton@umontreal.ca

Funding information
Environment and Climate Change Canada, Grant/Award Number: EDF-PQ-2020b012; Natural Resources Canada, Grant/Award Numbers: CWFC1718-018, CWFC1920-104; Natural Sciences and Engineering Research Council of Canada, Grant/Award Numbers: FEP RGPIN-2017-05452, STPGP-506680-17

Abstract

Soil contamination with toxic metalloids, such as arsenic, can represent a substantial human health and environmental risk. Some plants are thought to tolerate soil toxicity using root exudation, however, the nature of this response to arsenic remains largely unknown. Here, white lupin plants were exposed to arsenic in a semi-hydroponic system and their exudates were profiled using untargeted liquid chromatography-tandem mass spectrometry. Arsenic concentrations up to 1 ppm were tolerated and led to the accumulation of 12.9 μg As g^{-1} dry weight (DW) and 411 μg As g^{-1} DW in above-ground and belowground tissues, respectively. From 193 exuded metabolites, 34 were significantly differentially abundant due to 1 ppm arsenic, including depletion of glutathione disulphide and enrichment of phytochelatins and coumarins. Significant enrichment of phytochelatins in exudates of arsenic-treated plants was further confirmed using exudate sampling with strict root exclusion. The chemical tolerance toolkit in white lupin included nutrient acquisition metabolites as well as phytochelatins, the major intracellular metal-binding detoxification oligopeptides which have not been previously reported as having an extracellular role. These findings highlight the value of untargeted metabolite profiling approaches to reveal the unexpected and inform strategies to mitigate anthropogenic pollution in soils around the world.

KEYWORDS
arsenic, *Lupinus albus* (white lupin), metabolomics, phytochelatin, phytoremediation, rhizosphere, root exudates, stress tolerance

1 | INTRODUCTION

High arsenic concentrations can be naturally present in soil and groundwater but are also generated from anthropogenic industrial and agricultural activities (Han et al., 2003; Matschullat, 2000), which can damage the environment and cause risk to human health (Naujokas et al., 2013). In Canada, more than 7,000 arsenic and other metal(loid)-contaminated sites are listed as highly concerning by the Canadian government (Federal Contaminated Sites Inventory, 2019;

First Priority Substances List, 1988), but remediation is often hampered due to the high economic cost of conventional methods involving soil removal and burial. Some plants have evolved efficient arsenic tolerance mechanisms allowing them to colonize soils that are naturally high in arsenic concentrations (Meharg & Hartley-Whitaker, 2002), including translocation and accumulation into aerial biomass, as well as stabilization of arsenic in roots and soils (Raab et al., 2007). One way in which arsenic-contaminated soils could be rejuvenated is to exploit these natural plant mechanisms for

phytoremediation, the in-situ rehabilitation of soils by arsenic extraction or phytostabilization, as a sustainable alternative to more conventional remediation strategies (Pilon-Smits, 2005).

In aerobic soils, arsenic primarily occurs as the arsenate As(V) oxyanion (AsO_4^{3-}) which is an analogue of the phosphate oxyanion (PO_4^{3-}) and can be taken up by roots through phosphate transporters (Asher & Reay, 1979; Ullrich-Eberius et al., 1989). Once inside root cells, over 90% of As(V) can be reduced to As(III) by endogenous arsenate reductases (Chao et al., 2014; Dhankher et al., 2006). In anaerobic soils, arsenic primarily occurs as arsenite As(III), and can directly enter roots through aquaporins (Ma et al., 2008). Within root cells, As(III) can be translocated to other organs (Wang et al., 2018), extruded back into the soil (Xu et al., 2007; Zhao, Ago, et al., 2010), or form complexes with thiol (-SH) groups of oligopeptides, such as glutathione (γ-glutamate-cysteine-glycine: GSH) and phytochelatins ([γ-glutamate-cysteine]$_n$-glycine: PC$_n$), which can then be loaded into the vacuoles via ABC-type transporters (Li et al., 2016; Mishra et al., 2017; Raab et al., 2004; Schmöger et al., 2000; Song et al., 2014). As(III)-thiol complexation and compartmentalization in the vacuoles are considered as the main mechanisms for arsenic detoxification and stabilization in the roots of non-hyperaccumulating plant species (Zhao et al., 2009). Efflux of As(III) back into the soil is known to occur rapidly in *A. thaliana* and other non-hyperaccumulating species; while there is evidence that aquaporins play a partial role, explaining up to 20% of As(III) efflux (Zhao, Ago, et al., 2010), the major mechanisms explaining As(III) efflux in non-hyperaccumulators remain to be elucidated (Li et al., 2016; Zhao, McGrath, et al., 2010).

Interactions within the rhizosphere (the plant–soil interface) may also influence the fate of arsenic in contaminated soil as the bioavailability of metal(loid)s in soils can be strongly altered by plants (Dessureault-Rompré et al., 2008; Fresno et al., 2016; Fresno et al., 2017; Martínez-Alcalá et al., 2010). Plant influence on biochemistry within the rhizosphere is thought to be driven mainly through root exudation, which underlies important processes of nutrient acquisition and may also influence arsenic bioavailability (Fitz & Wenzel, 2002). However, despite the growing interest in understanding these mechanisms, relatively few studies have explored the interactions between root exudates and arsenic, partly due to the challenges in characterizing complex chemical mixtures within the rhizosphere (Oburger & Jones, 2018).

Root exudates are mainly composed of low molecular weight compounds such as carbohydrates, amino acids, phenolics, saponins, fatty acids and organic acids (OA) such as oxalate, malate and citrate, as well as other diverse and largely uncharacterized plant secondary metabolites (Strehmel et al., 2014; Tsuno et al., 2018; van Dam & Bouwmeester, 2016), which are known to collectively influence nutrient acquisition and interactions with microbes in the rhizosphere (Badri & Vivanco, 2009; Dakora & Phillips, 2002). OA exudates can alter the phosphate (P) soil bioavailability through ligand exchange, particularly in P-efficient crops such as white lupin (Dinkelaker et al., 1989; Neumann & Römheld, 1999; Wen et al., 2019). Phenolics such as flavonoids and coumarins are thought to help plants acquire

Fe through Fe(III) oxides reduction and complexation mechanisms (Cesco et al., 2010; Chen et al., 2017; Schmid et al., 2014). Studies have suggested that the recruitment and establishment of plant beneficial microorganisms is mediated by root exudates, such as genistein, an isoflavonoid involved in the symbiotic association of legumes and nitrogen-fixing bacteria (Kosslak et al., 1987; Liu & Murray, 2016; Schmidt, 1994). Similarly, saponins could help shape complex rhizosphere microbial communities and provide protection from pathogens and competing plants (Fujimatsu et al., 2020; Nakayasu et al., 2021; Oleszek & Jurzysta, 1987; Tsuno et al., 2018).

Despite the diversity of exuded compounds, only OAs are known to directly neutralize contaminants in the rhizosphere (Chen et al., 2017; Kochian, 1995; Lin & Aarts, 2012). Exuded OAs, such as oxalate, malate, citrate and nicotianamine can potentially form stable and non-phytotoxic complexes with metal(loid)s, and have been associated with tolerance to aluminium in *Phaseolus vulgaris* (Miyasaka et al., 1991; Ryan, 2001), cadmium in *Solanum lycopersicum* (Zhu et al., 2011) and zinc in *Arabidopsis halleri* (Tsednee et al., 2014). For arsenic, research has focussed on the arsenic hyperaccumulator *Pteris vittata* (Ma et al., 2001), which uses OA exudation to indirectly solubilize arsenic from As minerals and increase arsenic uptake (Das et al., 2017; Liu et al., 2017; Tu et al., 2004; Wu et al., 2018). However, less is known of root exudate adaptations to arsenic in non-hyperaccumulating species. For instance, some species of ferns and trees show a reduction in exuded OAs, amino acids and carbohydrates in the presence of arsenic (Johansson et al., 2008; Tu et al., 2004), while others have increased OA exudation (Mei et al., 2021). The extent and variation of root exudation in response to arsenic has yet to be examined in detail and plant species beyond *Pteris vittata* may possess unknown exudation mechanisms in response to arsenic.

To address this, the leguminous crop *Lupinus albus* (white lupin), with high tolerance to arsenic, high phosphate acquisition efficiency as well as extensive root exudation of organic acids and phenolics (Lambers et al., 2013; Vázquez et al., 2009; Weisskopf, Tomasi, et al., 2006) was subjected to a range of As(III) and As(V) concentrations within a controlled growth environment designed to capture exudates. Untargeted metabolite profiling was then used to elucidate the exudation response to successfully tolerated levels of arsenic.

2 | METHODS

2.1 | Experimental design, plant growth and arsenic quantification

White lupin seeds (*Lupinus albus* L. cv. AMIGA) were surface sterilize in consecutive baths of 70% ethanol, 1% sodium hypochlorite and sterile Milli-Q water. Seeds were germinated on sterile moist filter paper and seedlings were transferred to 7.6 × 15.2 cm 25 μm nylon mesh growth pouches containing 700 ml of washed and autoclaved silica sand as a growth medium (Figure 1). Plants were supplied twice a week with 65 ml Hoagland nutrient solution (1,600 μM N,
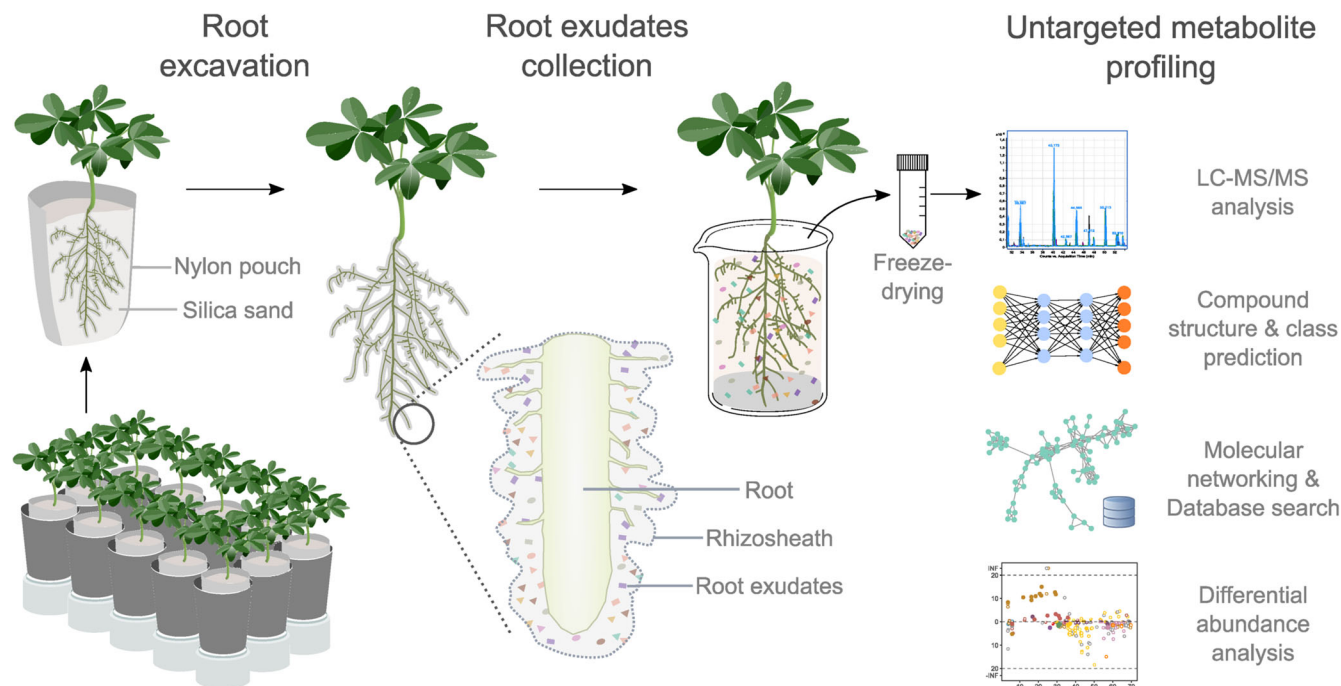
FIGURE 1 Root exudates analysis pipeline. Schematic view of an experimental block where each plant is excavated from the nylon pouch and the root system, with the rhizosheath containing root exudates, is dipped in water for 1 min to collect exudates. The trap solution is then freeze-dried to concentrate the analytes before LC–MS/MS analysis. Annotation steps include compound structure and class prediction using SIRIUS (Dührkop et al., 2019) and Feature-Based Molecular Networking in the GNPS environment (Nothias et al., 2020). Compound abundance (peak area) of plants treated with arsenic were compared to control plants to identify enriched and depleted exudates due to arsenic treatment [Colour figure can be viewed at wileyonlinelibrary.com]

200 μM P, 605 μM K, 400 μM Ca, 100.2 μM S, 100 μM Mg, 5 μM Cl, 2.5 μM B, 0.2 μM Mn, 0.2 μM Zn, 0.05 μM Cu, 0.05 μM Mo, 4.5 μM Fe) prepared with Milli-Q water and adjusted to pH 6 with sodium hydroxide 10%, when leachate was also collected beneath each growth pouch. Growth chamber conditions were LED lighting with photosynthetic light density of 150 μmol m^{-2} s^{-1}, a light/dark period of 18/6 h, temperature of 24.4 ± 0.2 / 22.5 ± 0.1°C, and 71.3 ± 2 / 76.3 ± 2% relative humidity.

After 21 days of growth, plants were either left as controls or exposed to one of five concentrations of either arsenite As(III), or arsenate As(V) added as sodium (meta)arsenite $NaAsO_2$ or sodium heptahydrate arsenate $Na_2HAsO_4 \cdot 7H_2O$. Treatments were applied five times at 2–3-day intervals until plants were harvested after 35 days of growth. Arsenic (element) concentrations were: 0 mg L^{-1} (control), 0.05 mg L^{-1} (0.7 μM), 0.1 mg L^{-1} (1.3 μM), 0.5 mg L^{-1} (6.7 μM), 1 mg L^{-1} (13.3 μM) and 5 mg L^{-1} (66.7 μM) and were prepared in Hoagland nutrient solution. A randomized block design was used with five replicate plants for each dose and each arsenic form (5 blocks, 60 plants in total). Unplanted controls were also included with the same treatments.

Signs of canopy toxicity and transpiration were monitored during growth, while root morphology, biomass production and arsenic concentrations were measured at harvest. Transpiration per plant (mL day^{-1}) was estimated as the difference of water loss in planted and unplanted control pots by day (Gu et al., 1996). Shoots and roots

were separated, roots were scanned (Epson, V750 PRO) and the images were processed with WinRHIZO (Regent Instruments Inc., Pornaro et al. 2017) for root surface area (RSA) measurements. Shoots and roots were then oven-dried at 105°C for 48 h and weighed. For total As quantification, dried shoots and roots, as well as reference material (NIST #1573a tomato leaf, for quality control), were ground and digested in nitric acid using a block digester for 6 h at 120°C and analysed by ICP-MS, following the methods described in Courchesne et al. (2017).

2.2 | Root exudate collection

Root exudate collection was performed based on Pearse et al. (2007), Ryan et al. (2012) and Wen et al. (2019), with minor modifications. Briefly, the nylon mesh growth pouches were cut open and loose sand was carefully removed from root systems to leave the attached rhizosheath. Root systems with the rhizosheath were then soaked in 40 mL Milli-Q water for 1 min with gentle circular shaking to capture exudates (Figure 1). Despite care taken to minimize root damage, the possibility that some exudates may originate from cellular damage cannot be excluded. Unplanted controls were extracted in the same conditions, by soaking approximately 20 g of sand collected from each unplanted pot, replicating a similar amount of sand extracted from rhizosheaths. The trap solutions were then lyophilized and stored at

−70°C. All lyophilized extracts were resuspended in 800 μL of Milli-Q water and filtered with 0.2 μm centrifuge filters prior to exudate profiling (InnoSep Spin, NY).

Validation of phytochelatin exudation used isolated exudates from belowground fractions to discount direct leaching from damaged root cells to the trap solution. The same experimental conditions were replicated but plants were only subjected to either 0.5 ppm arsenate or left as controls. Four different exudate sampling approaches were used: (1) standard rhizosphere extraction (RE) performed as described above, (2) rhizosheath (RS) extraction, (3) bulk soil (BS) extraction and (4) root exclusion (RX) extraction. The RS was isolated by careful collection of the sand attached to the root surface with a soft brush. BS comprised sand that was not attached to the root surface and was easily separated from the root system. RX samples, designed to strictly exclude root fragments, were collected using five heat-sealed 2.5 × 6 cm 25 μm nylon mesh pockets which were filled with sand and included in growth pouches before planting. At harvest, the nylon pockets were cut open and sand free from direct contact with roots, was collected. RS and RX sampling used 10 plants each, while the same 10 plants were used for RE and BS (30 plants in total). All samples were then extracted for root exuded metabolite profiling as described above.

2.3 | Low molecular weight organic acids analysis

Organic acids analysis was performed by HPLC on a Shimadzu SCL-10AVP equipped with an SIL-10AXL autosampler, LC-10VP pump, CTO-10ASvp Column Oven, RID-10A and SPD-10AV VP UV/Vis Detector at 254 nm. Organic acids from exudates or standards of citric acid and malic acid were separated using an AMINEX HPX-87H with isocratic elution of 0.005 M H_2SO_4 at 0.6 mL min^{-1} and column temperature of 65°C, based on Grierson (1992).

2.4 | Liquid chromatography-tandem mass spectrometry (LC–MS/MS) analysis

Chromatographic separation was performed using an Agilent 1,260 Infinity system, where 10 μL of exudate sample was injected onto a Zorbax Eclipse Plus C18 column (4.6 × 100 mm, 3.5 μm) at 30°C. *Mobile* phase was solvent A (water, 5% v/v methanol, 0.1% v/v formic acid) and solvent B (methanol, 0.1% formic acid) with a flow rate of 0.4 mL min^{-1} and an 80-minute elution gradient: 100% v/v A hold for 20 min, then a linear increase from 0% to 100% v/v B over 50 min and 100% v/v B hold for 10 min.

Untargeted full-scan (100–1,300 Da) MS1 acquisition was performed on biological samples (60 samples and 40 samples for phytochelatin validation) and controls (12 unplanted controls, and 5 blanks prepared from Milli-Q water) using an Agilent Q-TOF 6530B mass spectrometer equipped with an Agilent Jet Stream ion source operating in negative ion mode [ESI(−)]. Gas temperature was 300°C, drying gas flow was 5 L min^{-1} and the nebulizer pressure was 45 psig.

Sheath gas temperature was 250°C with a gas flow of 11 L min^{-1}. MS2 acquisition was performed on 12 representative samples (based on MS1 analysis) and blanks (samples extraction solvent and mobile phase). Tandem mass spectra were acquired with a collision energy of 20 and 35 V.

After LC–MS acquisition, raw data were processed using MZmine 2.37 (Pluskal et al., 2010). Background noise cut-off was set to an intensity threshold of 1,000 for MS1 and 500 for MS2. Chromatogram building was performed with a 10-ppm mass accuracy and a minimum peak intensity of 10,000. Extracted ion chromatograms were deconvoluted using MZmine minimum search algorithm. Isotope peaks were grouped with 10 ppm mass tolerance and 0.2 min retention time tolerance. Between samples, feature alignment was performed with 10 ppm mass tolerance (weighing for 80%) and 0.8 min retention time tolerance (weighing for 20%). Features that contained >1 isotope peak, and which occurred in >2 samples were retained. Gaps in the feature matrix were filled with 0.2 min retention time tolerance and 5 ppm mass tolerance. Features eluting in <0.2 min retention time windows and which peak shape correlated by >85% (Pearson correlation from MZmine meta-Correlate algorithm) were assigned to a feature group and used for curation of adducts, complex formation and in-source fragments, using the ion identity networking module in MZmine (Schmid et al., 2021). Features detected in >2 blank samples were removed from the dataset, while those detected in >6 unplanted controls were flagged. MS2 spectra were matched to a precursor ion from the MS1 chromatogram within 0.02 m/z and 0.2 min retention time windows. MS2 spectra from 20 and 35 eV collision energies matched to the same precursor ion were merged into a single consensus spectrum and their intensities summated. All retained features were between 3.5–69.8 min retention time (RT) and 115 to 1,087 *m/z*.

2.5 | Untargeted metabolite annotation

MS2 fragmentation spectra were annotated using feature-based molecular networking from the Global Natural Product Social Molecular Network (GNPS) platform (Nothias et al., 2020), as well as SIRIUS (version 4.5.3; Dührkop et al., 2019) for in silico formula, structure (Dührkop et al., 2015) and chemical class (Dührkop et al., 2020) prediction. Features annotation was further refined using the Plant Metabolic Network compound database of all available leguminous species (https://plantcyc.org/) (Caspi et al., 2018) and the public phytochelatin database PyCDB (Dennis et al., 2019) (https://kuppal.shinyapps.io/pycdb/), based on exact mass similarities (<5 ppm) and characteristic delta *m/z* of common adducts. For a limited number of features, annotation was confirmed from retention time and fragmentation spectra matching against standards (± 1 min RT, cosine >0.9). Standards included phytochelatin 2 (Anaspec, CA), glutathione (Alfa Aesar Co., Inc.), glutathione disulphide (ACROS Organics) and genistein (Sigma-Aldrich). Features with ambiguous annotation were annotated by best matching CANOPUS (Dührkop et al., 2020) predicted chemical class using ClassyFire taxonomy (Djoumbou Feunang et al., 2016). Annotation of each feature is categorized into four levels of metabolite

identification, as proposed standards for minimum reporting in metabolomics experiments (Sumner et al., 2007). Unless categorized as level 1 identification (identified from standards), all annotation should be considered as putative even when confirmed using database matched MS2 fragmentation patterns, as untargeted identification methodologies and database records are subject to change.

2.6 | Statistical analysis

All statistical tests were performed using R, version 4.0.2 (R Core Team, 2020). Comparisons of two groups were performed using Student's t-test and multiple groups comparisons were performed with ANOVA followed by Tukey HSD post hoc test ($\alpha < 0.05$). For differential abundance analysis of metabolic features, two groups comparisons were performed using Mann–Whitney U test with Benjamini-Hochberg correction, and multiple groups comparisons were performed using the non-parametric Kruskal-Wallis test [FSA package in R, (Ogle et al., 2020)], followed by Games-Howell post hoc test with Benjamini-Hochberg FDR correction [UFS package in R, (Peters, 2018)]. Diversity of features within exudate samples was estimated using Shannon and inverse Simpson indices (Schweiger et al., 2018), which account for both relative intensities and evenness between treatments. Unsupervised classification was estimated based on feature relative intensities using Bray–Curtis dissimilarity and the principal coordinates analysis (PCoA) ordination method. Dispersion ellipses used standard deviation for each treatment group. Significant distance was evaluated between the groups using the permutational multivariate analysis of variance (PERMANOVA) with Benjamini-Hochberg correction and permutations set to 9,999. Diversity and multivariate analysis were performed within the vegan R package (Oksanen et al., 2019).

3 | RESULTS

3.1 | Physiological response to arsenic

White lupin transpiration, above- and belowground biomass, RSA and above- and belowground As concentration did not significantly vary between plants when comparing As(III) to As(V) form at any specific concentration (t-test, $p > 0.05$; Data S1). When comparing the different As concentrations to controls (discounting form), transpiration of plants treated with 0.05, 0.1, 0.5 and 1 ppm As did not significantly vary from controls, with a mean transpiration of 7 ± 0.5 mL day^{-1} after the first As application (day 25) and 7.3 ± 0.7 mL day^{-1} before harvest (day 32), but some necrotic lesions were observed on leaves of plants treated with 1 ppm before harvest (Figure 2). Plants treated with 5 ppm As had a mean transpiration of 3.5 ± 0.3 mL day^{-1} after the first As application and a mean of 1.6 ± 0.2 mL day^{-1} before harvest, both of which were significantly lower than controls and other treatments (Tukey HSD, $\alpha < 0.05$). The first treatment with 5 ppm As also induced necrotic lesions in older leaves, which progressed to complete necrosis and abscission before harvest.

Mean above-ground dry weight was not significantly altered by 0.05, 0.1 and 0.5 ppm As when compared to control plants at a mean of 387.1 ± 16.3 mg, but was significantly lower in plants receiving 1 and 5 ppm As, at 307.6 ± 17 and 132.2 ± 10 mg, respectively (Figure 2). Belowground dry weight and RSA were not significantly altered by 0.05, 0.1, 0.5 and 1 ppm As compared to controls at a mean of 169.5 ± 15.5 mg and 143.5 ± 12.8 cm^2, but was significantly lower in plants receiving 5 ppm As, with 91.8 ± 8.6 mg and 52.4 ± 4 cm^2 (Tukey HSD, $\alpha < 0.05$).

Mean As concentrations in above-ground biomass of plants treated with 0.05, 0.1 and 0.5 ppm As were 1.7 ± 0.2, 2.4 ± 0.2, 7.3 ± 0.6 µg As g^{-1} dry weight (DW), respectively, and did not significantly differ from controls concentration of 0.3 ± 0.01 µg As g^{-1} DW (Figure 2). However, As concentrations were significantly higher than controls in above-ground biomass of plants treated with 1 ppm and 5 ppm As, with mean concentrations of 12.9 ± 1.9 and 46.9 ± 7.2 µg As g^{-1} DW, respectively (Tukey HSD, $\alpha < 0.05$). In belowground biomass, As concentrations were 11.7 ± 1 and 23.6 ± 1.2 µg As g^{-1} DW in plants treated with 0.05 and 0.1 ppm As, respectively, and increased in plants treated with 0.5, 1 and 5 ppm As, to concentrations of 171 ± 13.1, 411 ± 32.9 and 578.3 ± 34.8 µg As g^{-1} DW, which were significantly higher than 1.1 ± 1.1 µg As g^{-1} DW in controls (Tukey HSD, $\alpha < 0.05$).

3.2 | Organic acid exudation

Citric acid accumulation in the rhizosphere did not significantly vary in plants treated with 0.05, 0.1, 0.5 and 1 ppm As compared to controls, with a mean of 1.4 ± 0.2 mg citric acid g^{-1} root DW, but was significantly lower in plants receiving 5 ppm arsenic with 0.1 ± 0.04 mg citric acid g^{-1} root DW (Tukey HSD, $\alpha < 0.05$, Figure 2). Malic acid concentrations in the rhizosphere of plants treated with 0.05, 0.1 and 0.5 ppm As were 0.8 ± 0.3, 0.6 ± 0.2, 0.5 ± 0.2 mg malic acid g^{-1} root DW, respectively, and did not significantly differ from the concentration of controls with 1.2 ± 0.2 mg malic acid g^{-1} root DW. However, malic acid concentrations were significantly lower in plants receiving 1 and 5 ppm arsenic compared to controls, with mean concentrations of 0.3 ± 0.1 and 0.2 ± 0.1 mg malic acid g^{-1} root DW, respectively (Tukey HSD, $\alpha < 0.05$).

3.3 | Root exudate untargeted metabolite profile

The number of initial features per exudate sample ranged from 323 to 1,200. After alignment and quality control, which included the removal of one sample as an extreme outlier, a total of 245 features were retained as shared across >2 of the 59 root exudate samples (Figure 3). Of the 245 retained features, 82 were annotated as compounds, 80 annotated to a predicted chemical superclass, class, or subclass and 52 annotated as adducts, multimers and in-source fragments of identified metabolites (not considered in differential abundance analysis), while 31 features remained unknown (Data S1).
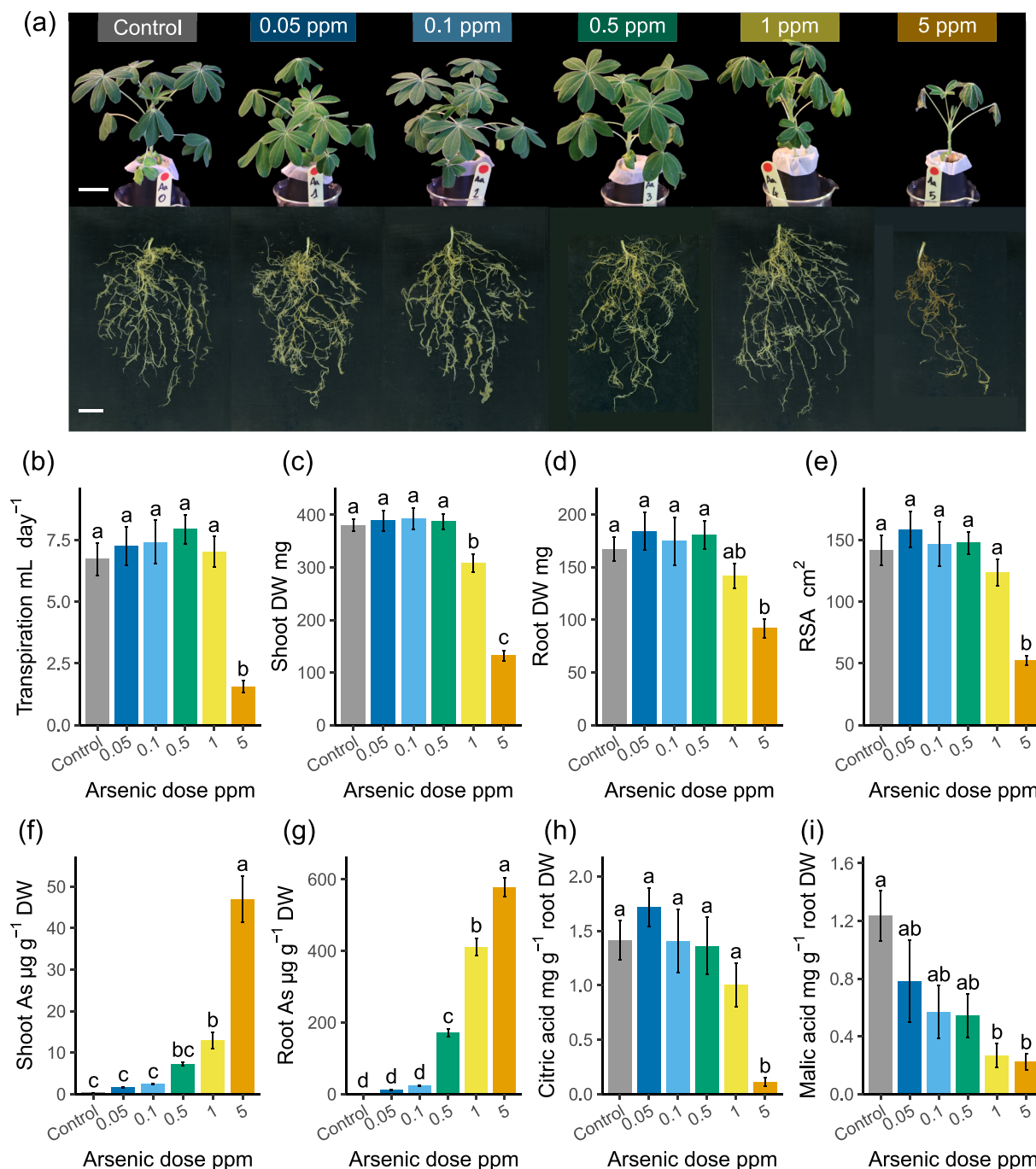
FIGURE 2 White lupin physiological parameters in response to arsenic. (a) Representative plant above-ground (top) and belowground (bottom) photographs before harvest in response to treatment (scale bars: 3 cm). Arsenic effect on (b) transpiration at harvest, (c, d) above-ground and belowground biomass, (e) root system area (RSA), (f, g) shoot and root arsenic concentrations, (h, i) root exudation of citric acid and malic acid. Data are means ± SE ($n = 10$). Different letters indicate significant differences (Tukey HSD, $\alpha < 0.05$) [Colour figure can be viewed at wileyonlinelibrary.com]

In total, root exudate features from controls and As exposed white lupin plants belonged to 15 predicted chemical classes, including: fatty acids, saponins, flavonoids, oligopeptides, coumarins, amino acids and derivatives, nucleosides and nucleotides, phenolic glycosides, benzenoids, carbohydrates, flavins, chalcones, lignans, hydroxycinnamic acids and carboxylic acids (Figure 3). Features with available fragmentation spectra were grouped into molecular networks based on spectral

similarity (cosine score > 0.4). This revealed 17 delimited subnetworks (clusters): the largest contained 55 features, the majority of which were flavonoids and coumarins and the second largest contained 18 features which were all oligopeptides (Figure 3). Forty-nine features did not cluster and were classified mostly as saponins or unknown features.

Using all 245 features across all samples, unsupervised analysis on Bray Curtis distances suggests samples separate by As dose and

FIGURE 3 Overview of untargeted metabolite profile of white lupin root exudates. (a) Quality control of untargeted LC–MS features. Each point represents a sample and bars represent means ± SE ($n = 60$ plants) before and after quality control filtering. (b) Number of compounds identified in the different chemical classes. (c) Molecular network based on MS2 spectra similarities (cosine >0.4) computed in the GNPS environment (Nothias et al., 2020) and plotted in Cytoscape, major cluster groups are circled. Full annotation of each feature is available in Data S1 [Colour figure can be viewed at wileyonlinelibrary.com]
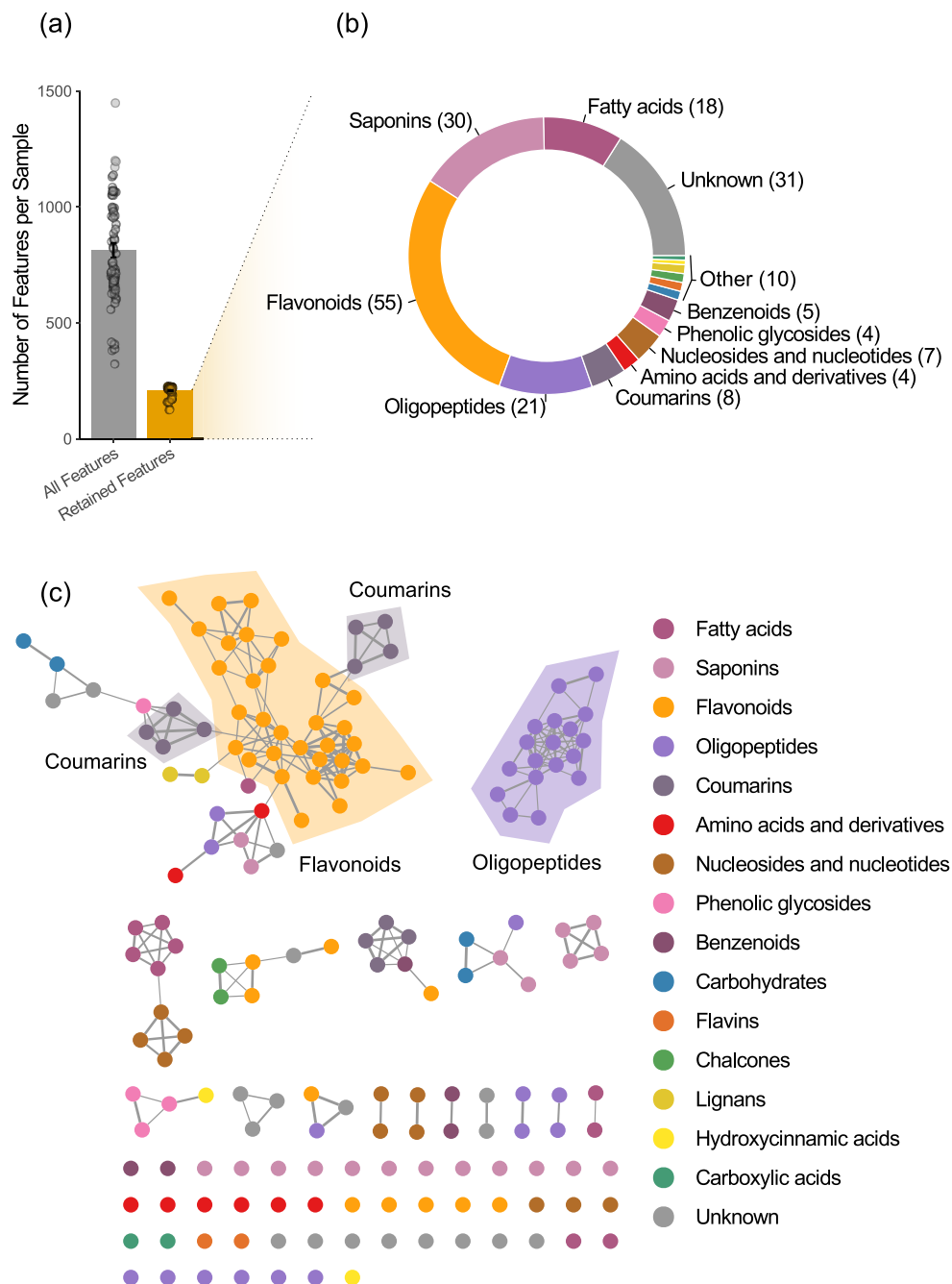
not by As form (Figure 4, Data S1). Permutational multivariate analysis of variance (PERMANOVA) revealed significantly greater variance between As doses than within dose ($p < 0.05$) and no significant difference between As(III) and As(V). Shannon and InvSimpson indices were used as a measure of feature diversity within samples; treatment with 5 ppm As significantly reduced both diversity indices compared to controls (Tukey HSD, $\alpha < 0.05$), while As form did not significantly alter either diversity indices.

Differential abundance analysis comparing As(III) and As(V) forms, within each As dose, revealed 11 significantly differentially abundant features (Data S1). Of these, 10 varied significantly at 0.1 ppm As and one feature varied significantly at 1 ppm As. Comparison between As doses (discounting form) to controls revealed a total of 93 significantly differentially abundant features in at least one As dose, with 73 depleted and 22 enriched (Figure 4). No significantly depleted features were detected at 0.05 or 0.1 ppm As, whereas one significantly depleted feature was detected at 0.5 ppm As, 14 at 1 ppm As and 73 at 5 ppm As. Significantly enriched features included three at 0.05 ppm As, six at 0.1 ppm As, 18 at 0.5 ppm As, 20 at 1 ppm As and 5 at 5 ppm As.

3.3.1 | Metabolites significantly altered between arsenic forms

Of the 11 features significantly differentially abundant between As forms, 10 were lower in 0.1 ppm As(III) compared to 0.1 ppm As(V),
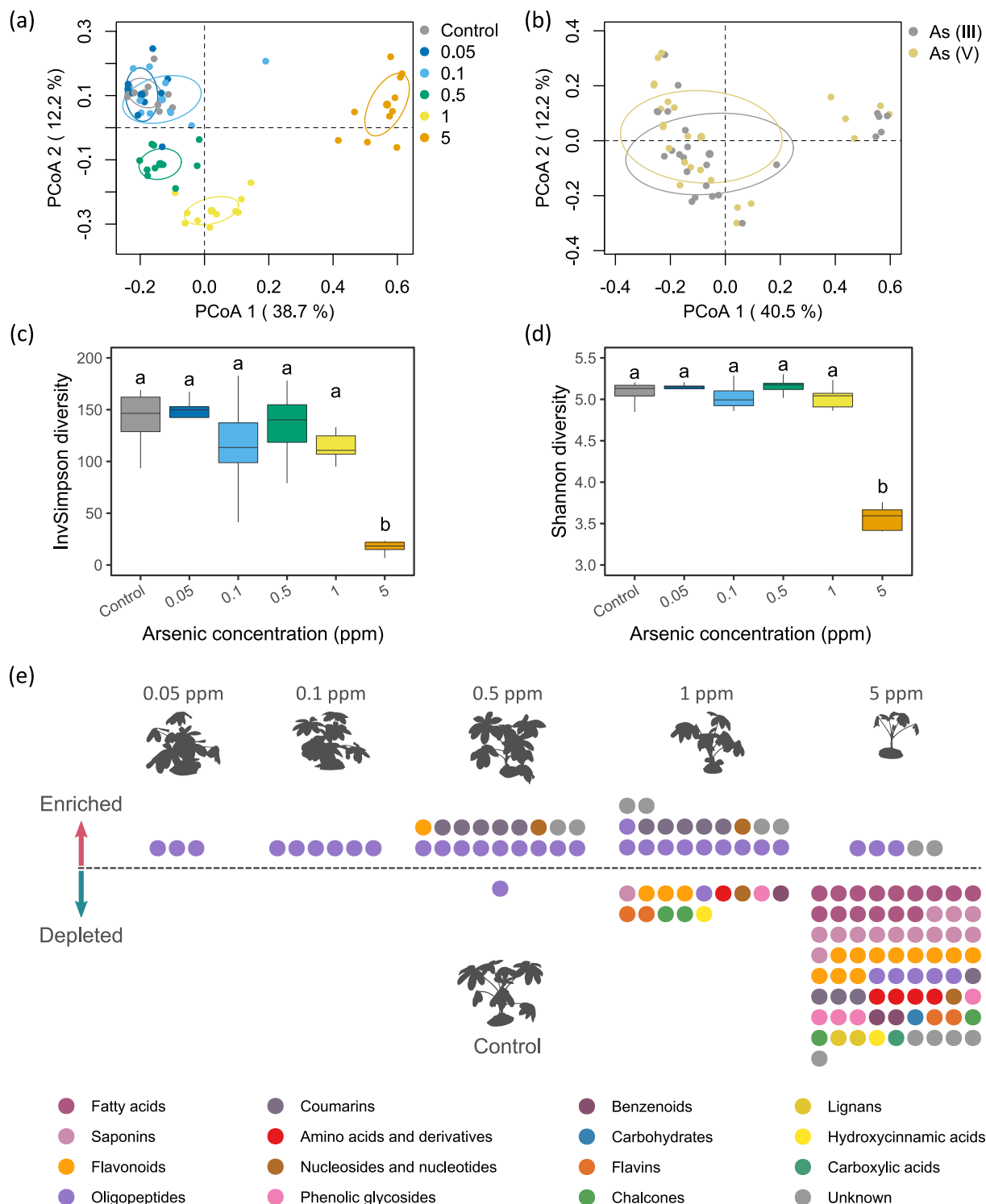
FIGURE 4 Alterations in white lupin root exudate profiles in response to arsenic. (a, b) PCoA of sample dissimilarity based on Bray-Curtis distances including standard deviation ellipses for treatment with arsenic doses or arsenic forms. (c, d) Shannon and InvSimpson diversity indices comparison between arsenic treatments, different letters indicate significant differences (Tukey HSD, $\alpha < 0.05$). (e) Significantly enriched and depleted features in the different arsenic concentrations compared to controls, each point represents one feature, coloured by chemical class [Colour figure can be viewed at wileyonlinelibrary.com]

and were putatively classified as six saponins, one flavonoid glycoside, one amino acid derivative, as well as two features that were unknown (Data S1). At 1 ppm, one feature, putatively classified as a

disaccharide, was significantly higher in As(III) compared to As(V). No significant differences were identified in exudates of plants treated with As(III) compared to As(V) at 0.05, 0.5 or 5 ppm As. Due to this

3.3.2 | Metabolites significantly altered by 5 ppm arsenic

The 73 features significantly depleted in response to 5 ppm As compared to controls were putatively classified into 15 chemical classes (Figure 4). The five largest depleted chemical classes were fatty acids (15), saponins (13), flavonoids (11), oligopeptides (5) and coumarins (4). The fatty acids included, trihydroxy octadecadienoic acids, trihydroxy octadecenoic acids and octadecynedioic acids, as well as one saccharolipid, licoagroside B (Data S1). The saponins included pisumsaponin II and soyasaponin I. Flavonoids included apigenin 6,8-digalactoside, apigenin 7-O-glucosylglucoside, apigenin 7-O-glucoside, dihydrokaempferol 7-glucoside and genistein glucoside. Oligopeptides included glutathione disulphide (GSSG). Coumarins included two chromenone glycoside derivatives. Other putative compounds included the amino acid, tryptophan, two flavins, riboflavin and lumiflavin, the phenolic glycosides p-coumaric acid glucoside and ferulic acid glucoside, the hydroxycinnamic acid, p-coumaric acid and the nucleoside uridine, while five significantly depleted features were unknown.

Of the five features enriched in response to 5 ppm As, three were classified as putative oligopeptides, including cysteineglutathione disulphide (CySSG), two yet-to-be-characterised compounds predicted as sulphur-containing gamma-glutamyl peptides (Feat_66, Feat_84, supp data), while the remaining two features were unknown (Figure 4, Data S1).

3.3.3 | Features significantly altered by 0.05, 0.1, 0.5 and 1 ppm arsenic

There was no significant depletion of exuded features in treatments with 0.05 and 0.1 ppm As when compared to controls. Treatment with 0.5 and 1 ppm As led to significant depletion of one and 14 features, respectively. The depleted feature in 0.5 ppm As treated plants was the oligopeptide GSSG, which was also depleted in response to 1 ppm, along with 13 other features from nine chemical classes: flavonoids (3), flavins (2), chalcones (2), amino acid derivatives (1), benzenoids (1), hydroxycinnamic acids (1), nucleosides (1), phenolic glycosides (1) and saponins (1) (Figures 4 and 5).

Exuded features significantly enriched in response to treatment with 0.05, 0.1, 0.5 and 1 ppm As when compared to controls belonged to four chemical classes, oligopeptides (10), coumarins (5), flavonoids (1), and nucleosides (1), while four features were unknown (Figures 4 and 5, Data S1). Treatment with 0.05 ppm As significantly enriched three putative oligopeptides: oxidized phytochelatin 2 (ox-PC$_2$), oxidized phytochelatin 2 with the glycine residue substituted for glutamic acid (ox-PC$_2$-Glu) as well as one uncharacterised sulphur-containing

gamma-glutamyl peptide (Feat_66, Data S1). Treatment with 0.1 ppm As also significantly enriched the common features ox-PC$_2$, ox-PC$_2$-Glu and the gamma-glutamyl peptide (Feat_66) along with three additional oligopeptides, oxidised PC$_2$ with a terminal glycine deletion (ox-DesGly-PC$_2$), one dimer of phytochelatin 3 (with three S—S bonds, [PC$_3$]$_2$), and one gamma-glutamyl peptide (Feat_84, isomer of Feat_66). Treatment with 0.5 ppm As significantly enriched, five coumarins, including four chromenone glycoside derivatives and one coumarin glycoside, one uncharacterized flavonoid, the nucleoside thymidine, the same oligopeptides ox-PC$_2$, ox-PC$_2$-Glu, ox-DesGly-PC$_2$, gamma-glutamyl peptides (Feat_66, Feat_84), the phytochelatin 3 dimer (PC$_3$)$_2$, as well as another phytochelatin 3 dimer, two phytochelatin 2 dimers (with two S—S bonds, [PC$_2$]$_2$), and two unknown features (Data S1). Treatment with 1 ppm As significantly enriched the same five coumarins, the nucleoside thymidine and the oligopeptides ox-PC$_2$, ox-PC$_2$-Glu, ox-DesGly-PC$_2$, gamma-glutamyl peptides (Feat_66, Feat_84), the two phytochelatin 3 dimers (PC$_3$)$_2$, two phytochelatin 2 dimers (PC$_2$)$_2$, cysteineglutathione disulphide (CySSG), and four unknown features (Figure 5). All enriched oligopeptides, except for (PC$_3$)$_2$, clustered into a single subnetwork (oligopeptide cluster; Figure 6) with similar fragmentation spectra (cosine score > 0.4) and which contained only one depleted metabolite, GSSG.

3.4 | Phytochelatins exudation validation

To further confirm exudation of phytochelatins, plants were treated with 0.5 ppm As or were left as controls, and different belowground fractions were sampled, including: root exclusion (RX), which was strictly isolated from direct contact with roots, rhizosheath (RS), bulk soil (BS) and rhizosphere (RE) as the standard exudate sampling approach (Figure 7). A total of 351 features were detected as shared across >2 exudate samples.

The phytochelatins and glutathione derivatives: ox-PC$_2$, ox-PC$_2$-Glu, ox-DesGly-PC$_2$, the two isomers of (PC$_2$)$_2$ and CySSG, were all significantly enriched in the RX belowground fraction from As-treated plants compared to controls (Figure 7), while only one phytochelatin 3 dimer (PC$_3$)$_2$ was detected in RX and did not significantly differ from controls. Conversely, GSSG was significantly depleted in the RX belowground fraction of As-treated plants compared to controls. Ox-PC$_2$, other PC variants and glutathione derivatives were also significantly increased in other belowground fractions when compared to controls, including the repeated standard rhizosphere extraction (RE), the rhizosheath (RS) and the bulk soil (BS) (Data S1).

Direct comparison between RE, RS, BS and RX belowground fractions of As-treated plants revealed ox-PC$_2$, ox-PC$_2$-Glu and ox-DesGly-PC$_2$ were higher in RE fractions when compared to RS fractions, which were higher compared to BS and RX fractions (Figure 7), consistent with an expected diffusion gradient. The two isomers of (PC$_3$)$_2$ were significantly higher in RE compared to BS and RX belowground fractions, but did not significantly differ between RS, BS and RX. GSSG and the two isomers of (PC$_2$)$_2$ were higher in RE and RS
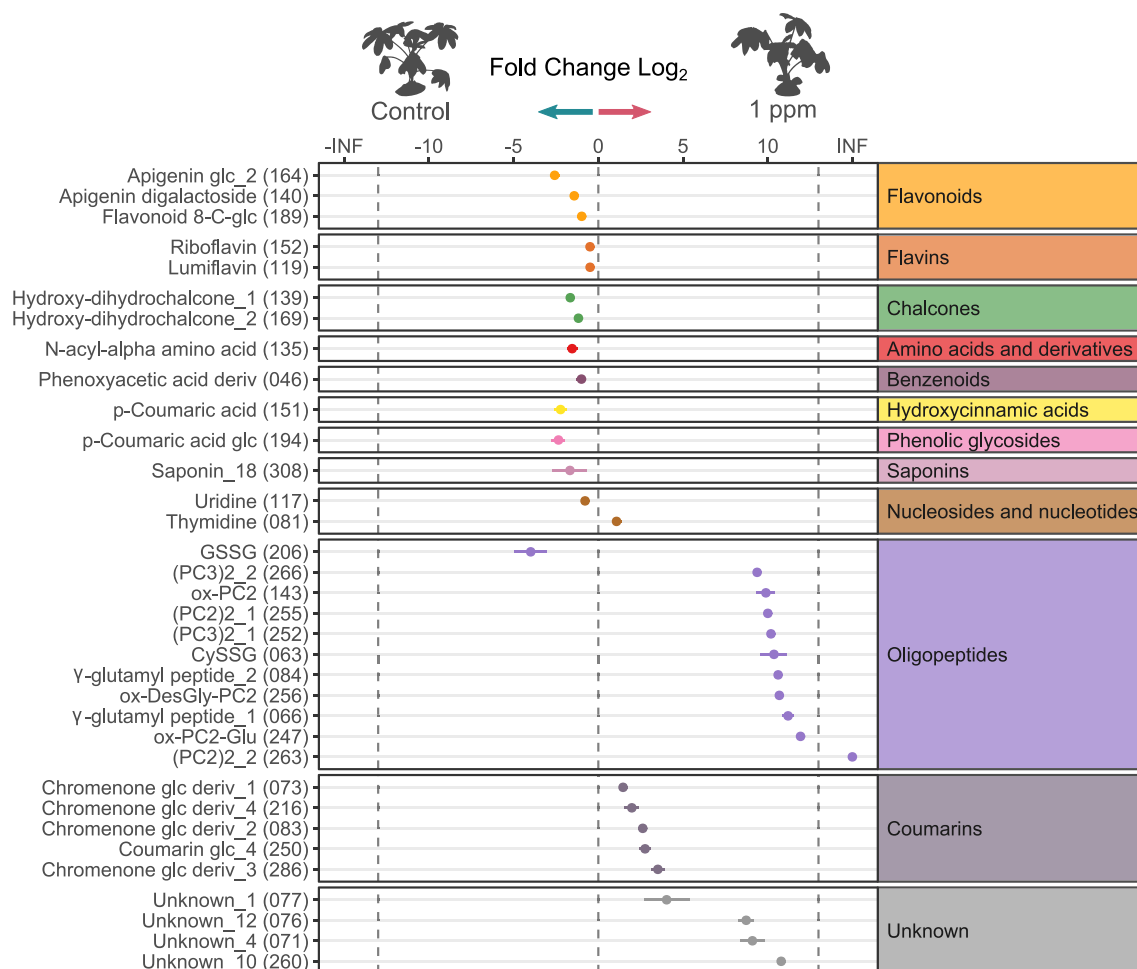
FIGURE 5 Differentially abundant exudates between plants treated with 1 ppm arsenic. Significantly differentially abundant exudates in 1 ppm arsenic compared to controls, annotated, and grouped by putative compound classes (Data S1 includes full annotation, feature unique ID is indicated in brackets). Statistical significance was determined using the non-parametric Kruskal-Wallis test, followed by Games-Howell post hoc test using a Benjamini-Hochberg correction (FDR adjusted $p < 0.05$). Data are mean fold change (FC $\log_2$) of peak intensities from significantly different exudates between arsenic-treated and control plants, ± SE ($n = 10$). The dashed lines indicate "infinite" fold change, where the exudate had detectable signal in only one condition [Colour figure can be viewed at wileyonlinelibrary.com]

fractions compared to BS and RX fractions, while CySSG remained stable between all belowground fractions.

4 | DISCUSSION

4.1 | Physiological response to arsenic

The absence of observed toxicity symptoms in canopy morphology, transpiration and biomass production in plants subjected to arsenic at concentrations of 0.05, 0.1 and 0.5 ppm suggests short-term tolerance to arsenic in white lupin within the semi-hydroponic system (Figure 1 and Figure 2). Visible toxicity symptoms on leaves after 11 days of treatment indicate a chronic toxic effect of 1 ppm arsenic, and similar symptoms after only 4 days of treatment indicate acute toxicity of 5 ppm arsenic. The leaf lesions in plants subjected to 5 ppm arsenic are characteristic of arsenic-induced oxidative stress (Sharma, 2012) and coincided with a

sharp decrease in transpiration and biomass production, consistent with impaired photosynthesis and primary metabolism due to arsenic cellular toxicity (Tripathi et al., 2012). Although arsenite As(III) and arsenate As(V) can have distinct degrees of phytotoxicity (Finnegan & Chen, 2012), they had similar effects on white lupin, potentially due to one form being rapidly converted to the other, as observed in rice and tomato by Xu et al. (2007), where >90% of As(V) was reduced into As(III) in the presence of plant roots. Treated plants significantly accumulated arsenic in both belowground and above-ground tissues, regardless of the arsenic form applied, in similar concentrations as those observed in hydroponically grown white lupin from Vázquez et al. (2005). The proportion of arsenic accumulated in roots was substantially higher than in shoots, with 76%–94% of the total arsenic retained in root systems. Preferential arsenic accumulation in roots was also highlighted in Vázquez et al. (2005, 2006), providing evidence that white lupin may be a good candidate for immobilizing arsenic within contaminated soils (a process termed "phytostabilisation").
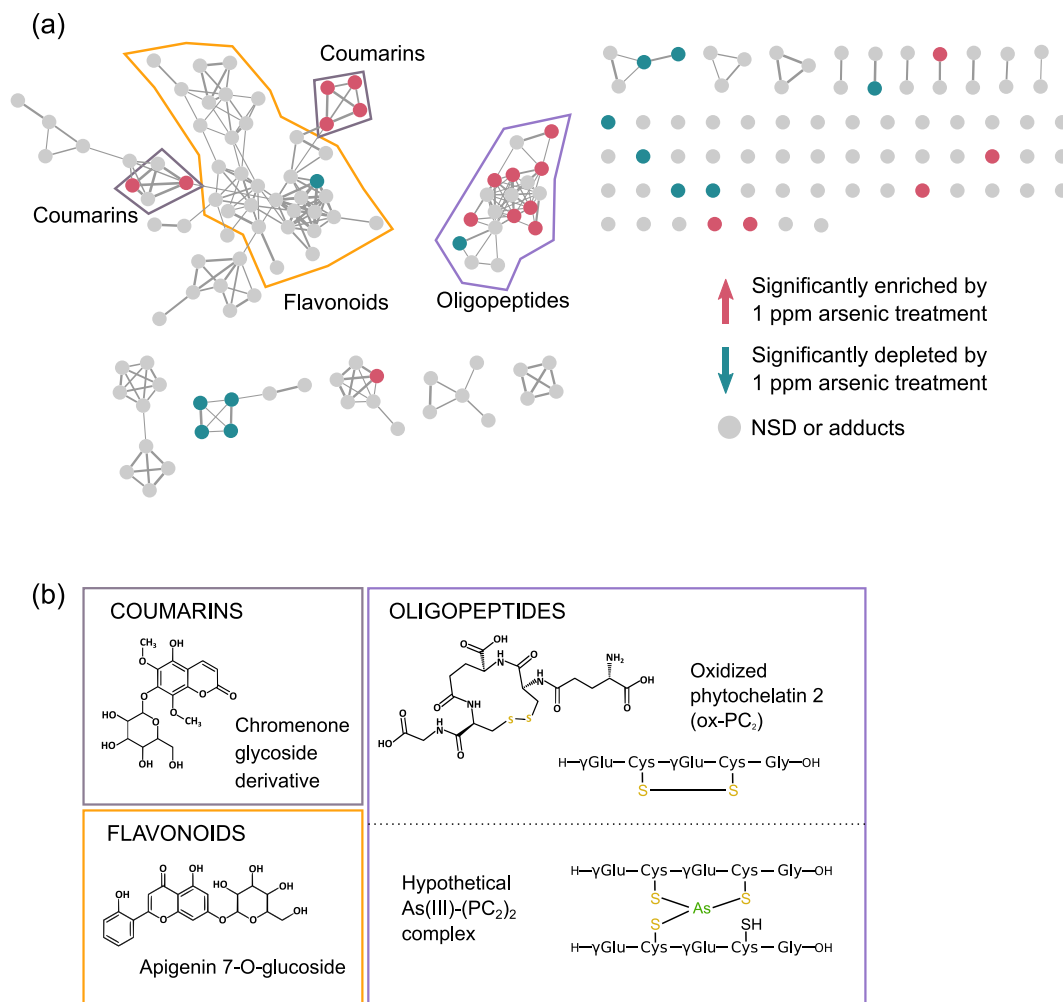
FIGURE 6 Molecular network and representative molecular structure of differentially abundant exudates in 1 ppm arsenic. (a) Molecular network of feature MS2 spectra similarities (cosine >0.4) computed in the GNPS environment (Nothias et al., 2020) and plotted in Cytoscape, major cluster groups are circled. Each significantly differentially abundant exudate is coloured by direction of significant change after 1 ppm arsenic treatment compared to controls (enriched in red, depleted in blue; NSD, non-significant difference). (b) Example molecular structures from major cluster groups from exudates, and hypothetical As(III)-(PC2)2 complex adapted from Schmöger et al. (2000) [Colour figure can be viewed at wileyonlinelibrary.com]

These results indicate that white lupin successfully tolerated concentrations up to 0.5 ppm of arsenic, had partial tolerance to 1 ppm arsenic and was sensitive to 5 ppm arsenic. This agrees with Moreno-Jiménez et al. (2010) where white lupin tolerated concentrations of 0.5 ppm As, which corresponded to the bioavailable arsenic from highly contaminated soil. White lupin response to arsenic is thought to involve root exudation of compounds, such as citric acid (Fresno et al., 2017). Here, citric acid and malic acid, the two main OAs found in root exudates of P-deficient white lupin (Neumann & Römheld, 1999; Pearse et al., 2007), were significantly reduced by high arsenic treatment, and were unaffected by tolerable arsenic levels. This suggests that white lupin might not use OA exudation to alter arsenic solubility directly within the rhizosphere, contrary to hyperaccumulating species such as *Pteris vittata* (Das et al., 2017; Liu et al., 2017; Tu et al., 2004). As the full range of exuded compounds in response to arsenic is largely unknown but

could influence the fate of soil arsenic, exuded compounds were profiled and compared.

4.2 | Root exudation is significantly altered in response to arsenic

Accurate exudate profiling is challenging due to the difficultly of sampling undamaged roots, the low concentrations, metabolite sorption onto soil particles, potential microbial interactions as well as other interfering soil constituents (Oburger & Jones, 2018). Semi-hydroponic silica sand cultivation systems, such as that used here (Pang et al., 2018; Pearse et al., 2007; Ryan et al., 2012; Sasse et al., 2020; Figure 1), enabled root exudates to be sampled from whole root systems for untargeted metabolite profiling. Overall, 245 exuded metabolites were repeatedly observed across multiple
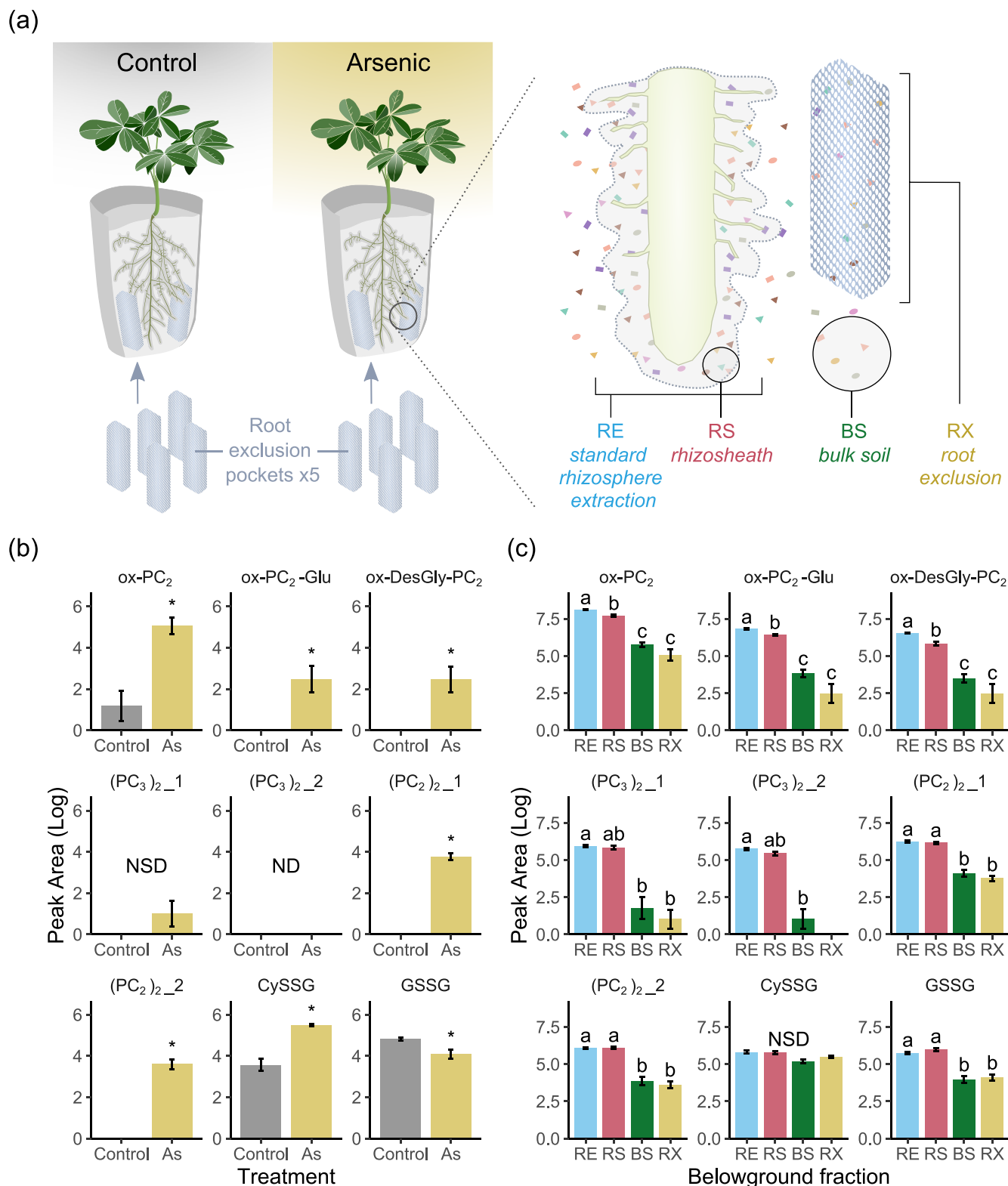
FIGURE 7 Validation of phytochelatin exudation. (a) Schematic of the rhizosphere of arsenic-treated and control plants illustrating different belowground fractions sampled for exudate profiling: Standard rhizosphere extraction (RE), rhizosheath (RS) extraction, bulk soil (BS) extraction, and root exclusion (RX) extraction. RX samples were collected using nylon mesh pockets filled with sand and included in growth pouches before planting which strictly exclude root penetration. (b) Phytochelatin and glutathione derivatives abundance (Log_{10} peak area) in RX belowground fraction from controls and arsenic-treated plants. Asterisks indicate significant difference from controls (Mann–Whitney U test, FDR adjusted $p < 0.05$). (c) Phytochelatin and glutathione derivatives abundance (Log_{10} peak area, normalised based on dry weight of extracted material) comparing the different belowground fractions of arsenic-treated plants. Data are means ± SE ($n = 5$ plants), different letters indicate significant difference (Games-Howell test, FDR adjusted $p < 0.05$). ND, non-detected; NSD, non-significant difference [Colour figure can be viewed at wileyonlinelibrary.com]

plants and arsenic drove significant and substantial changes in their abundance (based on peak intensities) when compared to untreated controls (Figure 4).

The form of arsenic had limited impact on exudation, with no significant differentially abundant metabolites detected between As(III) and As(V) at 0.05, 0.5 or 5 ppm. Only 10 metabolites identified as differentially abundant when comparing As(III) to As(V) at 0.1 ppm, including a relative reduction in saponins due to As(III), and one differentially abundant metabolite at 1 ppm. Saponins are commonly found in exudates of *Glycine max* and *Solanum lycopersicum*, where they are thought to alter rhizosphere microbial communities (Fujimatsu et al., 2020; Nakayasu et al., 2021). As comparative studies of As(III) and As(V) effects on plant metabolism are scarce (Tripathi et al., 2012), any direct role of altered saponin exudation or indirect interaction with rhizospheric microbiota is unclear.

Conversely, substantial differences in exudation profiles were induced between different arsenic doses when compared to untreated controls, with 93 differentially abundant metabolites in at least one dose when arsenic treatment (regardless of form) was compared to controls. The large proportion (78%) of differentially abundant metabolites significantly depleted in response to 5 ppm only (Figure 4) can likely be explained by a general decrease in metabolism and exudation, reflecting the physiological symptoms of arsenic sensitivity at this toxic concentration (Figure 2). In contrast, treatments with 0.05, 0.1, 0.5 and 1 ppm arsenic led to a more balanced shift in exuded metabolites, particularly in treatments with 0.5 ppm and 1 ppm (Figure 4), which were tolerated or partially tolerated by white lupin. The depletion of certain metabolites may reflect the action of intracellular arsenic toxicity but could also be a response aimed at decreasing arsenic sensitivity through a redirection of resources and switch from constitutive exudation to tolerance exudation. The corresponding significant enrichment of specific metabolites due to 0.5 and 1 ppm arsenic treatment likely represents the metabolites facilitating or directly acting towards neutralization of arsenic.

4.3 | Exudation profile of arsenic toxicity in white lupin

The toxicity response of white lupin to 5 ppm arsenic included a general decrease in metabolite exudation compared to controls (Figure 4, Data S1). These compounds were largely fatty acids, saponins and flavonoids, and are likely the constitutive white lupin root exudates associated to rhizosphere functions. For instance, the depleted fatty acids found here, such as trihydroxy octadecadienoic acids, have been reported in exudates of several species (da Silva Lima et al., 2014; Strehmel et al., 2014) including in white lupin (Lucas García et al., 2001), and can facilitate root penetration, nutrient exchange and microbial dynamics at the root soil interface as constituents of mucilage (McCully, 1999; Read et al., 2003). Other depleted fatty acids, such as octadecenoic acids, can be found in root hairs of *Glycine max* (a relative of lupin within Fabaceae), where they are thought to be involved in interactions with symbiotic rhizobacteria

(Brechenmacher et al., 2010). Saponins have also recently been identified in root exudates of *Glycine max* (Tsuno et al., 2018) and at high concentrations in roots of *Panax notoginseng* in arsenic contaminated soils (Zu et al., 2018). In addition, some saponins have been shown to protect mammalian cells from arsenic (Manna et al., 2007) and have been used as a biosurfactant to treat arsenic contaminated soils (Gusiatin, 2014). Flavonoids are commonly found in root exudates of white lupin and other species (Cesco et al., 2012) where they can have diverse functions. Amongst the flavonoids depleted in high arsenic here, apigenin glucoside is thought to be involved in legume-rhizobia interactions (Brechenmacher et al., 2010) and isoflavonoids such as genistein glucosides, have been found in white lupin rhizosphere as having antimicrobial activities and possible roles in Cu detoxification and P acquisition (Jung et al., 2003; Weisskopf, Abou-Mansour, et al., 2006; Weisskopf, Tomasi, et al., 2006). Alongside the symptoms of arsenic toxicity observed with 5 ppm arsenic (Figure 2), the depletion of these metabolites are therefore consistent with a reduction in root exudate functions, such as shaping soil physicochemical conditions through mucilage formation, improved nutrient acquisition, defence, as well as recruitment and maintenance of a healthy rhizosphere microbiome (Badri & Vivanco, 2009).

Although most exuded compounds were depleted in 5 ppm arsenic-treated white lupin, the arsenic toxicity also led to significant enrichment in three oligopeptides, cysteineglutathione disulphide (CySSG), and two sulphur-containing gamma-glutamyl peptides (Feat_66, Feat_84; Data S1) which clustered with CySSG within the oligopeptide cluster (Figure 3). Glutathione-derived sulphur-containing peptides such as these can be strongly induced during oxidative stress and metalloid response (Finnegan & Chen, 2012) and are consistent with the extreme toxicity of high arsenic concentrations.

4.4 | Exudation profile of arsenic tolerance in white lupin

Metabolites that were depleted in response to tolerated, or partially tolerated, levels of arsenic (0.5 and 1 ppm As) included, flavonoids, flavins, chalcones, amino acid derivatives, benzenoids, hydroxycinnamic acids, nucleosides, phenolic glycosides and saponins. Depletion in these diverse exudate molecular classes, which occurred mostly in response to 1 ppm arsenic, resembled the toxicity response to 5 ppm arsenic (Figure 4) and supports the physiological symptoms interpreted as partial tolerance of white lupin to 1 ppm arsenic (Figure 2). A common response to 0.5 and 1 ppm arsenic was the significant depletion in glutathione disulphide (GSSG). Previous research has provided evidence that GSSG can reduce translocation of metals such as cadmium to above-ground tissue (Nakamura et al., 2013). GSSG is the oxidized form of glutathione (GSH), a compound with high intracellular antioxidant activity (Jozefczak et al., 2012) which can form As(III)-GSH complexes like arsenotriglutathione in roots (Delnomdedieu et al., 1994; Raab et al., 2004; Raab et al., 2005). A reduction in GSSG within exudates after arsenic treatment could therefore be due to increased demand for GSH *in planta* for arsenic partitioning and

compartmentalization. Depleted intracellular levels of GSH due to arsenic have also previously been observed in lupin leaves, stems and roots, following the increased synthesis of phytochelatins (Vázquez et al., 2005). As GSH is difficult to capture in exudates due to high reactivity (Giustarini et al., 2016), the significant depletion of GSSG is an important clue suggesting a general redirection of the glutathione pathway towards increased synthesis and enrichment of arsenic tolerance exudates.

Enriched metabolites in root exudates due to arsenic belonged to four molecular classes, including 10 oligopeptides, five coumarins, one nucleoside, and one uncharacterized flavonoid. The nucleoside thymidine, a DNA constituent, has been shown to have exudate function as a growth substrate for rhizosphere microorganisms in *Avena barbata* (Zhalnina et al., 2018) and as a metabolite involved in response to P deficiency in *Glycine max* (Tawaraya et al., 2014). Enriched coumarins included four chromenone glycoside derivatives (Figure 5, Data S1), previously identified in root extracts from *Glycine max* (Zanzarin et al., 2020). The coumarin pathway was reported as up-regulated in response to Fe limitation in white lupin (Venuti et al., 2019) and some coumarins from *Arabidopsis* root exudates were shown to complex Fe (Schmid et al., 2014) but coumarins have not previously been associated to arsenic response, and their role in root exudates remain unclear. Arsenic is thought to cause Fe limitation in plants (Shaibur et al., 2009), therefore, enriched coumarin exudation could have a role in Fe nutrition during arsenic exposure to maintain lupin health.

Ten metabolites of the oligopeptide class were significantly enriched in response to tolerated levels of arsenic, and clustered to suggest related molecular structures (Figure 3 and Figure 6). Most of the enriched oligopeptides were identified as phytochelatins (PCs) or GSH-derived oligopeptides. As PC synthesis requires two GSH to form one phytochelatin 2 molecule (PC_2) (Grill et al., 1989; Scheller et al., 1987), the general enrichment of PCs within exudates could explain the depleted levels of total GSH (detected here as GSSG) in arsenic-treated plants due to a major shift in the glutathione pathway. The most abundant (based on peak intensities) form of exuded PCs was ox-PC_2, which is a major intracellular metal(loid) detoxification metabolite in plants, including white lupin, and is commonly identified in cells responding to different heavy metals and metal(loid)s such as lead, mercury, cadmium and arsenic (Cobbett & Goldsbrough, 2002; Vázquez et al., 2005). The two PCs, ox-PC_2-Glu and ox-DesGly-PC_2, have not previously been reported as detected in white lupin but are known metal(loid)-induced intracellular metabolites in tissues of other crops, such as rice (*Oryza sativa*) (Lemos Batista et al., 2014) and sunflower (*Helianthus annuus*) (Raab et al., 2005). To our knowledge, phytochelatins have not previously been reported in root exudates in any plant species.

4.5 | Phytochelatins exudation validation

To further confirm white lupin PC exudation in response to arsenic, an independent experiment was performed to strictly exclude roots from exudate samples (Figure 7). After arsenic treatment with 0.5 ppm, ox-PC_2, other PC variants, ox-PC_2-Glu, ox-DesGly-PC_2, ox-$(PC_2)_2$ and GSH-derivative CySSG were significantly enriched in the root exclusion (RX) fraction, which ensured complete separation of roots or roots fragments from the extracted sand using 25-μm nylon mesh pockets. Using the RX approach, the experimental results confirm the exudation of ox-PC_2, other PC variants and glutathione derivatives into the rhizosphere as opposed to these metabolites originating from root cell damage and leaching of intracellular metabolites during sampling.

All PCs decreased gradually from the surface of the roots (RE and RS) into the bulk soil (BS and RX) (Figure 7) in line with expected diffusion gradients of exuded compounds through soils (Dessureault-Rompré et al., 2006; Oburger et al., 2013) and confirms that the root zone of influence upon the soil, often considered as a definition of the rhizosphere, is spatially limited. A noteworthy exception was CySSG; present in similar abundance across all compartments, which suggests a high diffusion rate through the rhizosphere and is consistent with its short chromatographic retention time (3 min) due to strong polarity.

The diversity of PC variants enriched in exudates or arsenic treated plants suggests that white lupin could deploy an arsenal of detoxification metabolites directly in the rhizosphere (with roughly 53% of internal PC_2 levels exuded into the rhizosphere based on peak area per plant, Data S1). The major intracellular arsenic detoxification strategy in plants is thought to be the binding of As(III) to sulfhydryl (-SH) groups of PC cysteine residues in the cytoplasm to form a less toxic As(III)-PC complex (Schmöger et al., 2000). Complexation of arsenic with PC_2 has been directly observed in plants extracts, under specific buffer conditions, demonstrating the effective binding of one As(III) to three thiol (-SH) from two PC_2 molecules to form As(III)-$(PC_2)_2$ complexes (Raab et al., 2004; Schmöger et al., 2000; Figure 6). A similar arsenic detoxification mechanism by PCs could therefore operate within the rhizosphere directly to immobilize arsenic and reduce uptake into roots. Another hypothesis is that As(III)-$(PC_2)_2$ complexes are exuded (efflux) from roots as a mechanism to exclude arsenic in a similar manner as intracellular compartmentalization in plant vacuoles. Non-complexed arsenite efflux through channels of the NIP subfamily of plant aquaporins has been reported in several species but only explains up to 20% of total As(III) efflux from roots into the soil in non-hyperaccumulators, where 50%–100% of intracellular As(III) is complexed with thiols (Bienert et al., 2008; Li et al., 2016; Ma et al., 2008; Zhao, Ago, et al., 2010, 2009). Interestingly, Song et al. (2014) reported the expression of rice ABC-type transporters, responsible for As(III)-PC loading into the vacuole, within the plasma membrane of the root epidermis, providing a route for efflux of As(III)-PC complexes into the rhizosphere.

5 | CONCLUSIONS

Untargeted metabolite profiling revealed white lupin has a distinctive root exudate response to arsenic. The exudation profile associated with successful tolerance of high arsenic concentrations included unexpected compounds, such as coumarins, several yet-to-be-

characterized molecules and a diverse suite of phytochelatins, exudation that was further confirmed through repeated growth trials and strict exclusion of roots from sampled growth medium. These findings provide evidence that an extracellular arsenic tolerance mechanism mediated by phytochelatins exists in white lupin which has the potential to explain the successful tolerance of excluder species. This improved understanding of how plants can adapt to, and potentially alter, metal(loid) challenged soil environments can help inform sustainable strategies to help mitigate environmental pollution.

CONFLICT OF INTEREST

The authors declare that they have no conflict of interest.

DATA AVAILABILITY STATEMENT

The data that supports the findings of this study are available in the supplementary material of this article

ORCID

Adrien Frémont https://orcid.org/0000-0003-1956-6517
Eszter Sas https://orcid.org/0000-0001-7677-7906
Emmanuel Gonzalez https://orcid.org/0000-0002-5567-2125
Jacques Brisson https://orcid.org/0000-0003-0046-7551
Frédéric Emmanuel Pitre https://orcid.org/0000-0003-2104-6940
Nicholas James Beresford Brereton https://orcid.org/0000-0002-2434-3249

REFERENCES

Asher, C. J., & Reay, P. F. (1979). Arsenic uptake by barley seedlings. *Functional Plant Biology*, 6, 459–466. https://doi.org/10.1071/pp9790459

Badri, D. V., & Vivanco, J. M. (2009). Regulation and function of root exudates. *Plant, Cell & Environment*, 32, 666–681. https://doi.org/10.1111/j.1365-3040.2009.01926.x

Bienert, G. P., Thorsen, M., Schüssler, M. D., Nilsson, H. R., Wagner, A., Tamás, M. J., & Jahn, T. P. (2008). A subgroup of plant aquaporins facilitate the bi-directional diffusion of as(OH)3 and Sb(OH)3across membranes. *BMC Biology*, 6, 26. https://doi.org/10.1186/1741-7007-6-26

Brechenmacher, L., Lei, Z., Libault, M., Findley, S., Sugawara, M., Sadowsky, M. J., ... Stacey, G. (2010). Soybean metabolites regulated in root hairs in response to the symbiotic bacterium *Bradyrhizobium japonicum*. *Plant Physiology*, 153, 1808–1822. https://doi.org/10.1104/pp.110.157800

Caspi, R., Billington, R., Fulcher, C. A., Keseler, I. M., Kothari, A., Krummenacker, M., ... Karp, P. D. (2018). The MetaCyc database of metabolic pathways and enzymes. *Nucleic Acids Research*, 46, D633–D639. https://doi.org/10.1093/nar/gkx935

Cesco, S., Mimmo, T., Tonon, G., Tomasi, N., Pinton, R., Terzano, R., ... Nannipieri, P. (2012). Plant-borne flavonoids released into the rhizosphere: Impact on soil bio-activities related to plant nutrition. A review. *Biology and Fertility of Soils*, 48, 123–149. https://doi.org/10.1007/s00374-011-0653-2

Cesco, S., Neumann, G., Tomasi, N., Pinton, R., & Weisskopf, L. (2010). Release of plant-borne flavonoids into the rhizosphere and their role in plant nutrition. *Plant and Soil*, 329, 1–25. https://doi.org/10.1007/s11104-009-0266-9

Chao, D.-Y., Chen, Y., Chen, J., Shi, S., Chen, Z., Wang, C., ... Salt, D. E. (2014). Genome-wide association mapping identifies a new arsenate reductase enzyme critical for limiting arsenic accumulation in plants. *PLoS Biology*, 12, e1002009. https://doi.org/10.1371/journal.pbio.1002009

Chen, Y.-T., Wang, Y., & Yeh, K.-C. (2017). Role of root exudates in metal acquisition and tolerance. *Current Opinion in Plant Biology*, 39, 66–72. https://doi.org/10.1016/j.pbi.2017.06.004

Cobbett, C., & Goldsbrough, P. (2002). Phytochelatins and metallothioneins: Roles in heavy metal detoxification and homeostasis. *Annual Review of Plant Biology*, 53, 159–182. https://doi.org/10.1146/annurev.arplant.53.100301.135154

Courchesne, F., Turmel, M.-C., Cloutier-Hurteau, B., Constantineau, S., Munro, L., & Labrecque, M. (2017). Phytoextraction of soil trace elements by willow during a phytoremediation trial in southern Québec, Canada. *International Journal of Phytoremediation*, 19, 545–554. https://doi.org/10.1080/15226514.2016.1267700

da Silva Lima, L., Olivares, F. L., Rodrigues de Oliveira, R., Vega, M. R. G., Aguiar, N. O., & Canellas, L. P. (2014). Root exudate profiling of maize seedlings inoculated with *Herbaspirillum seropedicae* and humic acids. *Chemical and Biological Technologies in Agriculture*, 1, 23. https://doi.org/10.1186/s40538-014-0023-z

Dakora, F. D., & Phillips, D. A. (2002). Root exudates as mediators of mineral acquisition in low-nutrient environments. *Plant and Soil*, 245, 35–47. https://doi.org/10.1023/A:1020809400075

Das, S., Chou, M.-L., Jean, J.-S., Yang, H.-J., & Kim, P. J. (2017). Arsenic-enrichment enhanced root exudates and altered rhizosphere microbial communities and activities in hyperaccumulator *Pteris vittata*. *Journal of Hazardous Materials*, 325, 279–287. https://doi.org/10.1016/j.jhazmat.2016.12.006

Delnomdedieu, M., Basti, M. M., Otvos, J. D., & Thomas, D. J. (1994). Reduction and binding of arsenate and dimethylarsinate by glutathione: A magnetic resonance study. *Chemico-Biological Interactions*, 90, 139–155. https://doi.org/10.1016/0009-2797(94)90099-X

Dennis, K. K., Uppal, K., Liu, K. H., Ma, C., Liang, B., Go, Y.-M., & Jones, D. P. (2019). Phytochelatin database: A resource for phytochelatin complexes of nutritional and environmental metals. *Database, Journal of Biological Databases Curation*, 2019. https://doi.org/10.1093/database/baz083

Dessureault-Rompré, J., Nowack, B., Schulin, R., & Luster, J. (2006). Modified micro suction cup/rhizobox approach for the in-situ detection of organic acids in rhizosphere soil solution. *Plant and Soil*, 286, 99–107. https://doi.org/10.1007/s11104-006-9029-z

Dessureault-Rompré, J., Nowack, B., Schulin, R., Tercier-Waeber, M.-L., & Luster, J. (2008). Metal solubility and speciation in the rhizosphere of *Lupinus albus* cluster roots. *Environmental Science & Technology*, 42, 7146–7151. https://doi.org/10.1021/es800167g

Dhankher, O. P., Rosen, B. P., McKinney, E. C., & Meagher, R. B. (2006). Hyperaccumulation of arsenic in the shoots of Arabidopsis silenced for arsenate reductase (ACR2). *Proceedings of the National Academy of Sciences*, 103, 5413–5418. https://doi.org/10.1073/pnas.0509770102

Dinkelaker, B., Römheld, V., & Marschner, H. (1989). Citric acid excretion and precipitation of calcium citrate in the rhizosphere of white lupin (*Lupinus albus* L.). *Plant, Cell & Environment*, 12, 285–292. https://doi.org/10.1111/j.1365-3040.1989.tb01942.x

Djoumbou Feunang, Y., Eisner, R., Knox, C., Chepelev, L., Hastings, J., Owen, G., … Wishart, D. S. (2016). ClassyFire: Automated chemical classification with a comprehensive, computable taxonomy. *Journal of Cheminformatics*, 8, 61. https://doi.org/10.1186/s13321-016-0174-y

Dührkop, K., Fleischauer, M., Ludwig, M., Aksenov, A. A., Melnik, A. V., Meusel, M., … Böcker, S. (2019). SIRIUS 4: A rapid tool for turning tandem mass spectra into metabolite structure information. *Nature Methods*, 16, 299–302. https://doi.org/10.1038/s41592-019-0344-8

Dührkop, K., Nothias, L.-F., Fleischauer, M., Reher, R., Ludwig, M., Hoffmann, M. A., … Böcker, S. (2020). Systematic classification of unknown metabolites using high-resolution fragmentation mass spectra. *Nature Biotechnology*, 1–10, 462–471. https://doi.org/10.1038/s41587-020-0740-8

Dührkop, K., Shen, H., Meusel, M., Rousu, J., & Böcker, S. (2015). Searching molecular structure databases with tandem mass spectra using CSI: FingerID. *Proceedings of the National Academy of Sciences*, 112, 12580–12585. https://doi.org/10.1073/pnas.1509788112

Federal Contaminated Sites Inventory. (2019). Treasury Board of Canada Secretariat. https://www.tbs-sct.gc.ca/fcsi-rscf/home-accueil.aspx. Accessed 2021.

Finnegan, P., & Chen, W. (2012). Arsenic toxicity: The effects on plant metabolism. *Frontiers in Physiology*, 3. https://doi.org/10.3389/fphys.2012.00182

First Priority Substances List. (1988). Health Canada. https://www.canada.ca/en/health-canada/services/environmental-workplace-health/reports-publications/environmental-contaminants/first-priority-substances-list-psl1-assessments-priority-substances-assessment-program-environmental-contaminants.html. Accessed 2021.

Fitz, W. J., & Wenzel, W. W. (2002). Arsenic transformations in the soil–rhizosphere–plant system: Fundamentals and potential application to phytoremediation. *Journal of Biotechnology*, 99, 259–278. https://doi.org/10.1016/S0168-1656(02)00218-3

Fresno, T., Peñalosa, J. M., Santner, J., Puschenreiter, M., & Moreno-Jiménez, E. (2017). Effect of *Lupinus albus* L. root activities on As and Cu mobility after addition of iron-based soil amendments. *Chemosphere*, 182, 373–381. https://doi.org/10.1016/j.chemosphere.2017.05.034

Fresno, T., Peñalosa, J. M., Santner, J., Puschenreiter, M., Prohaska, T., & Moreno-Jiménez, E. (2016). Iron plaque formed under aerobic conditions efficiently immobilizes arsenic in *Lupinus albus* L roots. *Environmental Pollution*, 216, 215–222. https://doi.org/10.1016/j.envpol.2016.05.071

Fujimatsu, T., Endo, K., Yazaki, K., & Sugiyama, A. (2020). Secretion dynamics of soyasaponins in soybean roots and effects to modify the bacterial composition. *Plant Direct*, 4, e00259. https://doi.org/10.1002/pld3.259

Giustarini, D., Tsikas, D., Colombo, G., Milzani, A., Dalle-Donne, I., Fanti, P., & Rossi, R. (2016). Pitfalls in the analysis of the physiological antioxidant glutathione (GSH) and its disulfide (GSSG) in biological samples: An elephant in the room. *Journal of Chromatography B, Analytical Tools and Protocols in Oxidative Stress*, 1019, 21–28. https://doi.org/10.1016/j.jchromb.2016.02.015

Grierson, P. F. (1992). Organic acids in the rhizosphere of *Banksia integrifolia* L.f. *Plant and Soil*, 144, 259–265. https://doi.org/10.1007/BF00012883

Grill, E., Löffler, S., Winnacker, E.-L., & Zenk, M. H. (1989). Phytochelatins, the heavy-metal-binding peptides of plants, are synthesized from glutathione by a specific γ-glutamylcysteine dipeptidyl transpeptidase (phytochelatin synthase). *Proceedings of the National Academy of Sciences*, 86, 6838–6842. https://doi.org/10.1073/pnas.86.18.6838

Gu, S. L., Fuchigami, L. H., Guak, S. H., & Shin, C. (1996). Effects of short-term water stress, hydrophilic polymer amendment, and antitranspirant on stomatal status, transpiration, water loss, and growth in "better boy" tomato plants. *Journal of the American Society for Horticultural Science*, 121, 831–837. https://doi.org/10.21273/JASHS.121.5.831

Gusiatin, Z. M. (2014). Tannic acid and saponin for removing arsenic from brownfield soils: Mobilization, distribution and speciation. *Journal of Environmental Sciences*, 26, 855–864. https://doi.org/10.1016/S1001-0742(13)60534-3

Han, F. X., Su, Y., Monts, D. L., Plodinec, M. J., Banin, A., & Triplett, G. E. (2003). Assessment of global industrial-age anthropogenic arsenic contamination. *Naturwissenschaften*, 90, 395–401. https://doi.org/10.1007/s00114-003-0451-2

Johansson, E. M., Fransson, P. M. A., Finlay, R. D., & van Hees, P. A. W. (2008). Quantitative analysis of root and ectomycorrhizal exudates as a response to Pb, Cd and As stress. *Plant and Soil*, 313, 39–54. https://doi.org/10.1007/s11104-008-9678-1

Jozefczak, M., Remans, T., Vangronsveld, J., & Cuypers, A. (2012). Glutathione is a key player in metal-induced oxidative stress defenses. *International Journal of Molecular Sciences*, 13, 3145–3175. https://doi.org/10.3390/ijms13033145

Jung, C., Maeder, V., Funk, F., Frey, B., Sticher, H., & Frossard, E. (2003). Release of phenols from *Lupinus albus* L. roots exposed to Cu and their possible role in Cu detoxification. *Plant and Soil*, 252, 301–312. https://doi.org/10.1023/A:1024775803759

Kochian, L. V. (1995). Cellular mechanisms of aluminum toxicity and resistance in plants. *Annual Review of Plant Physiology and Plant Molecular Biology*, 46, 237–260. https://doi.org/10.1146/annurev.pp.46.060195.001321

Kosslak, R. M., Bookland, R., Barkei, J., Paaren, H. E., & Appelbaum, E. R. (1987). Induction of *Bradyrhizobium japonicum* common nod genes by isoflavones isolated from *Glycine max*. *Proceedings of the National Academy of Sciences*, 84, 7428–7432. https://doi.org/10.1073/pnas.84.21.7428

Lambers, H., Clements, J. C., & Nelson, M. N. (2013). How a phosphorus-acquisition strategy based on carboxylate exudation powers the success and agronomic potential of lupines (Lupinus, Fabaceae). *American Journal of Botany*, 100, 263–288. https://doi.org/10.3732/ajb.1200474

Lemos Batista, B., Nigar, M., Mestrot, A., Alves Rocha, B., Barbosa Júnior, F., Price, A. H., … Feldmann, J. (2014). Identification and quantification of phytochelatins in roots of rice to long-term exposure: Evidence of individual role on arsenic accumulation and translocation. *Journal of Experimental Botany*, 65, 1467–1479. https://doi.org/10.1093/jxb/eru018

Li, N., Wang, J., & Song, W.-Y. (2016). Arsenic uptake and translocation in plants. *Plant & Cell Physiology*, 57, 4–13. https://doi.org/10.1093/pcp/pcv143

Lin, Y.-F., & Aarts, M. G. M. (2012). The molecular mechanism of zinc and cadmium stress response in plants. *Cellular and Molecular Life Sciences*, 69, 3187–3206. https://doi.org/10.1007/s00018-012-1089-z

Liu, C.-W., & Murray, J. D. (2016). The role of flavonoids in nodulation host-range specificity: An update. *Plants*, 5, 33. https://doi.org/10.3390/plants5030033

Liu, X., Fu, J., Da Silva, E., Shi, X., Cao, Y., Rathinasabapathi, B., … Ma, L. Q. (2017). Microbial siderophores and root exudates enhanced goethite dissolution and Fe/As uptake by as-hyperaccumulator *Pteris vittata*. *Environmental Pollution*, 223, 230–237. https://doi.org/10.1016/j.envpol.2017.01.016

Lucas García, J. A., Barbas, C., Probanza, A., Barrientos, M. L., & Gutierrez Mañero, F. J. (2001). Low molecular weight organic acids and fatty acids in root exudates of two Lupinus cultivars at flowering and fruiting stages. *Phytochemical Analysis PCA*, 12, 305–311. https://doi.org/10.1002/pca.596

Ma, J. F., Yamaji, N., Mitani, N., Xu, X.-Y., Su, Y.-H., McGrath, S. P., & Zhao, F.-J. (2008). Transporters of arsenite in rice and their role in arsenic accumulation in rice grain. *Proceedings of the National Academy of Sciences*, 105, 9931–9935. https://doi.org/10.1073/pnas.0802361105

Ma, L. Q., Komar, K. M., Tu, C., Zhang, W., Cai, Y., & Kennelley, E. D. (2001). A fern that hyperaccumulates arsenic. *Nature*, 409, 579–579. https://doi.org/10.1038/35054664

Manna, P., Sinha, M., Pal, P., & Sil, P. C. (2007). Arjunolic acid, a triterpenoid saponin, ameliorates arsenic-induced cyto-toxicity in hepatocytes. *Chemico-Biological Interactions*, 170, 187–200. https://doi.org/10.1016/j.cbi.2007.08.001

Martínez-Alcalá, I., Walker, D. J., & Bernal, M. P. (2010). Chemical and biological properties in the rhizosphere of *Lupinus albus* alter soil heavy metal fractionation. *Ecotoxicology and Environmental Safety*, 73, 595–602. https://doi.org/10.1016/j.ecoenv.2009.12.009

Matschullat, J. (2000). Arsenic in the geosphere—A review. *Science of the Total Environment*, 249, 297–312. https://doi.org/10.1016/S0048-9697(99)00524-0

McCully, M. E. (1999). ROOTS IN SOIL: Unearthing the complexities of roots and their rhizospheres. *Annual Review of Plant Physiology and Plant Molecular Biology*, 50, 695–718. https://doi.org/10.1146/annurev.arplant.50.1.695

Meharg, A. A., & Hartley-Whitaker, J. (2002). Arsenic uptake and metabolism in arsenic resistant and nonresistant plant species: Tansley review no. 133. *The New Phytologist*, 154, 29–43. https://doi.org/10.1046/j.1469-8137.2002.00363.x

Mei, K., Liu, J., Fan, J., Guo, X., Wu, J., Zhou, Y., … Yan, C. (2021). Low-level arsenite boosts rhizospheric exudation of low-molecular-weight organic acids from mangrove seedlings (*Avicennia marina*): Arsenic phytoextraction, removal, and detoxification. *Science of the Total Environment*, 775, 145685. https://doi.org/10.1016/j.scitotenv.2021.145685

Mishra, S., Mattusch, J., & Wennrich, R. (2017). Accumulation and transformation of inorganic and organic arsenic in rice and role of thiol-complexation to restrict their translocation to shoot. *Scientific Reports*, 7, 40522. https://doi.org/10.1038/srep40522

Miyasaka, S. C., Buta, J. G., Howell, R. K., & Foy, C. D. (1991). Mechanism of aluminum tolerance in snapbeans: Root exudation of citric acid. *Plant Physiology*, 96, 737–743. https://doi.org/10.1104/pp.96.3.737

Moreno-Jiménez, E., Esteban, E., Fresno, T., López de Egea, C., & Peñalosa, J. M. (2010). Hydroponics as a valid tool to assess arsenic availability in mine soils. *Chemosphere*, 79, 513–517. https://doi.org/10.1016/j.chemosphere.2010.02.034

Nakamura, S., Suzui, N., Nagasaka, T., Komatsu, F., Ishioka, N. S., Ito-Tanabata, S., … Fujimaki, S. (2013). Application of glutathione to roots selectively inhibits cadmium transport from roots to shoots in oilseed rape. *Journal of Experimental Botany*, 64, 1073–1081. https://doi.org/10.1093/jxb/ers388

Nakayasu, M., Ohno, K., Takamatsu, K., Aoki, Y., Yamazaki, S., Takase, H., … Sugiyama, A. (2021). Tomato roots secrete tomatine to modulate the bacterial assemblage of the rhizosphere. *Plant Physiology*, 186, 270–284. https://doi.org/10.1093/plphys/kiab069

Naujokas, M. F., Beth, A., Habibul, A., Vasken, A. H., Graziano, J. H., Claudia, T., & Suk, W. A. (2013). The broad scope of health effects from chronic arsenic exposure: Update on a worldwide public health problem. *Environmental Health Perspectives*, 121, 295–302. https://doi.org/10.1289/ehp.1205875

Neumann, G., & Römheld, V. (1999). Root excretion of carboxylic acids and protons in phosphorus-deficient plants. *Plant and Soil*, 211, 121–130. https://doi.org/10.1023/A:1004380832118

Nothias, L.-F., Petras, D., Schmid, R., Dührkop, K., Rainer, J., Sarvepalli, A., … Dorrestein, P. C. (2020). Feature-based molecular networking in the GNPS analysis environment. *Nature Methods*, 17, 905–908. https://doi.org/10.1038/s41592-020-0933-6

Oburger, E., Dell'mour, M., Hann, S., Wieshammer, G., Puschenreiter, M., & Wenzel, W. W. (2013). Evaluation of a novel tool for sampling root exudates from soil-grown plants compared to conventional techniques. *Environmental and Experimental Botany*, 87, 235–247. https://doi.org/10.1016/j.envexpbot.2012.11.007

Oburger, E., & Jones, D. L. (2018). Sampling root exudates—Mission impossible? *Rhizosphere*, 6, 116–133. https://doi.org/10.1016/j.rhisph.2018.06.004

Ogle, D., Wheeler, P., Dinno, A., 2020. *FSA: Fisheries Stock Analysis (Version 0.8. 30, R package)*.

Oksanen, J., Blanchet, F.G., Friendly, M., Kindt, R., Legendre, P., McGlinn, D., Minchin, P.R., O'Hara, R.B., Simpson, G.L., Solymos, P., Stevens, M.H.H., Szoecs, E., Wagner, H., 2019. vegan: Community Ecology Package.

Oleszek, W., & Jurzysta, M. (1987). The allelopathic potential of alfalfa root medicagenic acid glycosides and their fate in soil environments. *Plant and Soil*, 98, 67–80. https://doi.org/10.1007/BF02381728

Pang, J., Bansal, R., Zhao, H., Bohuon, E., Lambers, H., Ryan, M. H., … Siddique, K. H. M. (2018). The carboxylate-releasing phosphorus-mobilizing strategy can be proxied by foliar manganese concentration in a large set of chickpea germplasm under low phosphorus supply. *The New Phytologist*, 219, 518–529. https://doi.org/10.1111/nph.15200

Pearse, S. J., Veneklaas, E. J., Cawthray, G., Bolland, M. D. A., & Lambers, H. (2007). Carboxylate composition of root exudates does not relate consistently to a crop species' ability to use phosphorus from aluminium, iron or calcium phosphate sources. *The New Phytologist*, 173, 181–190. https://doi.org/10.1111/j.1469-8137.2006.01897.x

Peters, G.-J., 2018. Userfriendlyscience (UFS): Quantitative analysis made accessible. https://doi.org/10.17605/OSF.IO/TXEQU

Pilon-Smits, E. (2005). Phytoremediation. *Annual Review of Plant Biology*, 56, 15–39. https://doi.org/10.1146/annurev.arplant.56.032604.144214

Pluskal, T., Castillo, S., Villar-Briones, A., & Orešič, M. (2010). MZmine 2: Modular framework for processing, visualizing, and analyzing mass spectrometry-based molecular profile data. *BMC Bioinformatics*, 11, 395. https://doi.org/10.1186/1471-2105-11-395

Pornaro, C., Macolino, S., Menegon, A., & Richardson, M. (2017). WinRHIZO technology for measuring morphological traits of bermudagrass stolons. *Agronomy Journal*, 109(6), 3007–3010. http://dx.doi.org/10.2134/agronj2017.03.0187

R Core team. (2020). R: A language and environment for statistical computing. Vienna, Austria: R Foundation for Statistical Computing. URL https://www.R-project.org/

Raab, A., Feldmann, J., & Meharg, A. A. (2004). The nature of arsenic-phytochelatin complexes in *Holcus lanatus* and *Pteris cretica*. *Plant Physiology*, 134, 1113–1122. https://doi.org/10.1104/pp.103.033506

Raab, A., Schat, H., Meharg, A. A., & Feldmann, J. (2005). Uptake, translocation and transformation of arsenate and arsenite in sunflower (*Helianthus annuus*): Formation of arsenic-phytochelatin complexes during exposure to high arsenic concentrations. *The New Phytologist*, 168, 551–558. https://doi.org/10.1111/j.1469-8137.2005.01519.x

Raab, A., Williams, P. N., Meharg, A., & Feldmann, J. (2007). Uptake and translocation of inorganic and methylated arsenic species by plants. *Environment and Chemistry*, 4, 197–203. https://doi.org/10.1071/EN06079

Read, D. B., Bengough, A. G., Gregory, P. J., Crawford, J. W., Robinson, D., Scrimgeour, C. M., … Zhang, X. (2003). Plant roots release phospholipid surfactants that modify the physical and chemical properties of soil. *The New Phytologist*, 157, 315–326. https://doi.org/10.1046/j.1469-8137.2003.00665.x

Ryan, M. H., Tibbett, M., Edmonds-Tibbett, T., Suriyagoda, L. D. B., Lambers, H., Cawthray, G. R., & Pang, J. (2012). Carbon trading for phosphorus gain: The balance between rhizosphere carboxylates and

arbuscular mycorrhizal symbiosis in plant phosphorus acquisition. *Plant, Cell & Environment*, 35, 2170–2180. https://doi.org/10.1111/j.1365-3040.2012.02547.x

Ryan, P. R., Delhaize, E., & Jones, D. L. (2001). Function and mechanism of organic anion exudation from plant roots. *Annual Review of Plant Physiology and Plant Molecular Biology*, 52, 527–560. https://doi.org/10.1146/annurev.arplant.52.1.527

Sasse, J., Kosina, S. M., de Raad, M., Jordan, J. S., Whiting, K., Zhalnina, K., & Northen, T. R. (2020). Root morphology and exudate availability are shaped by particle size and chemistry in *Brachypodium distachyon*. *Plant Direct*, 4, e00207. https://doi.org/10.1002/pld3.207

Scheller, H. V., Huang, B., Hatch, E., & Goldsbrough, P. B. (1987). Phytochelatin synthesis and glutathione levels in response to heavy metals in tomato cells. *Plant Physiology*, 85, 1031–1035. https://doi.org/10.1104/pp.85.4.1031

Schmid, N. B., Giehl, R. F. H., Döll, S., Mock, H.-P., Strehmel, N., Scheel, D., ... von Wirén, N. (2014). Feruloyl-CoA 6′-Hydroxylase1-dependent coumarins mediate iron acquisition from alkaline substrates in Arabidopsis. *Plant Physiology*, 164, 160–172. https://doi.org/10.1104/pp.113.228544

Schmid, R., Petras, D., Nothias, L.-F., Wang, M., Aron, A. T., Jagels, A., ... Dorrestein, P. C. (2021). Ion identity molecular networking in the GNPS environment. *bioRxiv*. 12(1), 1–2. https://doi.org/10.1101/2020.05.11.088948

Schmidt, P. E. (1994). Nod factors of *Bradyrhizobium japonicum* and Rhizobium sp. NGR234 induce flavonoid accumulation in soybean root exudate. *Molecular Plant-Microbe Interactions*, 7, 384. https://doi.org/10.1094/MPMI-7-0384

Schmöger, M. E. V., Oven, M., & Grill, E. (2000). Detoxification of arsenic by phytochelatins in plants. *Plant Physiology*, 122, 793–802.

Schweiger, A. K., Cavender-Bares, J., Townsend, P. A., Hobbie, S. E., Madritch, M. D., Wang, R., ... Gamon, J. A. (2018). Plant spectral diversity integrates functional and phylogenetic components of biodiversity and predicts ecosystem function. *Nature Ecology and Evolution*, 2, 976–982. https://doi.org/10.1038/s41559-018-0551-1

Shaibur, M. R., Kitajima, N., Huq, S. M. I., & Kawai, S. (2009). Arsenic–iron interaction: Effect of additional iron on arsenic-induced chlorosis in barley grown in water culture. *Soil Science & Plant Nutrition*, 55, 739–746. https://doi.org/10.1111/j.1747-0765.2009.00414.x

Sharma, I. (2012). Arsenic induced oxidative stress in plants. *Biologia (Bratisl.)*, 67, 67–453. https://doi.org/10.2478/s11756-012-0024-y

Song, W.-Y., Yamaki, T., Yamaji, N., Ko, D., Jung, K.-H., Fujii-Kashino, M., ... Ma, J. F. (2014). A rice ABC transporter, OsABCC1, reduces arsenic accumulation in the grain. *Proceedings of the National Academy of Sciences*, 111, 15699–15704. https://doi.org/10.1073/pnas.1414968111

Strehmel, N., Böttcher, C., Schmidt, S., & Scheel, D. (2014). Profiling of secondary metabolites in root exudates of *Arabidopsis thaliana*. *Phytochemistry*, 108, 35–46. https://doi.org/10.1016/j.phytochem.2014.10.003

Sumner, L. W., Amberg, A., Barrett, D., Beale, M. H., Beger, R., Daykin, C. A., ... Viant, M. R. (2007). Proposed minimum reporting standards for chemical analysis. *Metabolomics*, 3, 211–221. https://doi.org/10.1007/s11306-007-0082-2

Tawaraya, K., Horie, R., Shinano, T., Wagatsuma, T., Saito, K., & Oikawa, A. (2014). Metabolite profiling of soybean root exudates under phosphorus deficiency. *Soil Science & Plant Nutrition*, 60, 679–694. https://doi.org/10.1080/00380768.2014.945390

Tripathi, R. D., Tripathi, P., Dwivedi, S., Dubey, S., Chakrabarty, D., & Trivedi, P. K. (2012). Arsenomics: Omics of arsenic metabolism in plants. *Frontiers in Physiology*, 3, 275. https://doi.org/10.3389/fphys.2012.00275

Tsednee, M., Yang, S.-C., Lee, D.-C., & Yeh, K.-C. (2014). Root-secreted nicotianamine from Arabidopsis halleri facilitates zinc hypertolerance by regulating zinc bioavailability. *Plant Physiology*, 166, 839–852. https://doi.org/10.1104/pp.114.241224

Tsuno, Y., Fujimatsu, T., Endo, K., Sugiyama, A., & Yazaki, K. (2018). Soyasaponins: A new class of root exudates in soybean (*Glycine max*). *Plant & Cell Physiology*, 59, 366–375. https://doi.org/10.1093/pcp/pcx192

Tu, S., Ma, L., & Luongo, T. (2004). Root exudates and arsenic accumulation in arsenic hyperaccumulating Pteris vittata and non-hyperaccumulating *Nephrolepis exaltata*. *Plant and Soil*, 258, 9–19. https://doi.org/10.1023/B:PLSO.0000016499.95722.16

Ullrich-Eberius, C. I., Sanz, A., & Novacky, A. J. (1989). Evaluation of arsenate- and vanadate-associated changes of electrical membrane potential and phosphate transport in Lemna gibba G1. *Journal of Experimental Botany*, 40, 119–128. https://doi.org/10.1093/jxb/40.1.119

van Dam, N. M., & Bouwmeester, H. J. (2016). Metabolomics in the rhizosphere: Tapping into belowground chemical communication. *Trends in Plant Science*, 21, 256–265. https://doi.org/10.1016/j.tplants.2016.01.008

Vázquez, S., Agha, R., Granado, A., Sarro, M. J., Esteban, E., Peñalosa, J. M., & Carpena, R. O. (2006). Use of white lupin plant for phytostabilization of Cd and As polluted acid soil. *Water, Air, and Soil Pollution*, 177, 349–365. https://doi.org/10.1007/s11270-006-9178-y

Vázquez, S., Esteban, E., & Goldsbrough, P. (2005). Arsenate-induced phytochelatins in white lupin: Influence of phosphate status. *Physiologia Plantarum*, 124, 41–49. https://doi.org/10.1111/j.1399-3054.2005.00484.x

Vázquez, S., Goldsbrough, P., & Carpena, R. O. (2009). Comparative analysis of the contribution of phytochelatins to cadmium and arsenic tolerance in soybean and white lupin. *Plant Physiology and Biochemistry*, 47, 63–67. https://doi.org/10.1016/j.plaphy.2008.09.010

Venuti, S., Zanin, L., Marroni, F., Franco, A., Morgante, M., Pinton, R., & Tomasi, N. (2019). Physiological and transcriptomic data highlight common features between iron and phosphorus acquisition mechanisms in white lupin roots. *Plant Science*, 285, 110–121. https://doi.org/10.1016/j.plantsci.2019.04.026

Wang, C., Na, G., Bermejo, E. S., Chen, Y., Banks, J. A., Salt, D. E., & Zhao, F.-J. (2018). Dissecting the components controlling root-to-shoot arsenic translocation in *Arabidopsis thaliana*. *The New Phytologist*, 217, 206–218. https://doi.org/10.1111/nph.14761

Weisskopf, L., Abou-Mansour, E., Fromin, N., Tomasi, N., Santelia, D., Edelkott, I., ... Martinoia, E. (2006). White lupin has developed a complex strategy to limit microbial degradation of secreted citrate required for phosphate acquisition. *Plant, Cell & Environment*, 29, 919–927. https://doi.org/10.1111/j.1365-3040.2005.01473.x

Weisskopf, L., Tomasi, N., Santelia, D., Martinoia, E., Langlade, N. B., Tabacchi, R., & Abou-Mansour, E. (2006). Isoflavonoid exudation from white lupin roots is influenced by phosphate supply, root type and cluster-root stage. *The New Phytologist*, 171, 657–668. https://doi.org/10.1111/j.1469-8137.2006.01776.x

Wen, Z., Li, H., Shen, Q., Tang, X., Xiong, C., Li, H., ... Shen, J. (2019). Tradeoffs among root morphology, exudation and mycorrhizal symbioses for phosphorus-acquisition strategies of 16 crop species. *The New Phytologist*, 223, 882–895. https://doi.org/10.1111/nph.15833

Wu, F., Xu, F., Ma, X., Luo, W., Lou, L., & Wong, M. H. (2018). Do arsenate reductase activities and oxalate exudation contribute to variations of arsenic accumulation in populations of *Pteris vittata*? *Journal of Soils and Sediments*, 18, 1–9. https://doi.org/10.1007/s11368-018-1987-2

Xu, X. Y., McGrath, S. P., & Zhao, F. J. (2007). Rapid reduction of arsenate in the medium mediated by plant roots. *The New Phytologist*, 176, 590–599. https://doi.org/10.1111/j.1469-8137.2007.02195.x

Zanzarin, D. M., Hernandes, C. P., Leme, L. M., Silva, E., Porto, C., Martin do Prado, R., ... Pilau, E. J. (2020). Metabolomics of soybean green stem and foliar retention (GSFR) disease using mass spectrometry and

molecular networking. *Rapid Communications in Mass Spectrometry, RCM, 34*(Suppl 3), e8655. https://doi.org/10.1002/rcm.8655

Zhalnina, K., Louie, K. B., Hao, Z., Mansoori, N., da Rocha, U. N., Shi, S., … Brodie, E. L. (2018). Dynamic root exudate chemistry and microbial substrate preferences drive patterns in rhizosphere microbial community assembly. *Nature Microbiology, 1*, 470–480. https://doi.org/10.1038/s41564-018-0129-3

Zhao, F.-J., Ago, Y., Mitani, N., Li, R.-Y., Su, Y.-H., Yamaji, N., … Ma, J. F. (2010). The role of the rice aquaporin Lsi1 in arsenite efflux from roots. *The New Phytologist, 186*, 392–399. https://doi.org/10.1111/j.1469-8137.2010.03192.x

Zhao, F. J., Ma, J. F., Meharg, A. A., & McGrath, S. P. (2009). Arsenic uptake and metabolism in plants. *The New Phytologist, 181*, 777–794. https://doi.org/10.1111/j.1469-8137.2008.02716.x

Zhao, F.-J., McGrath, S. P., & Meharg, A. A. (2010). Arsenic as a food chain contaminant: Mechanisms of plant uptake and metabolism and mitigation strategies. *Annual Review of Plant Biology, 61*, 535–559. https://doi.org/10.1146/annurev-arplant-042809-112152

Zhu, X. F., Zheng, C., Hu, Y. T., Jiang, T., Liu, Y., Dong, N. Y., … Zheng, S. J. (2011). Cadmium-induced oxalate secretion from root apex is associated with cadmium exclusion and resistance in *Lycopersicon esulentum*.

Plant, Cell & Environment, 34, 1055–1064. https://doi.org/10.1111/j.1365-3040.2011.02304.x

Zu, Y., Li, Z., Mei, X., Wu, J., Cheng, S., Jiang, Y., & Li, Y. (2018). Transcriptome analysis of main roots of *Panax notoginseng* identifies genes involved in saponin biosynthesis under arsenic stress. *Plant Gene, 16*, 1–7. https://doi.org/10.1016/j.plgene.2018.08.001

SUPPORTING INFORMATION

Additional supporting information may be found in the online version of the article at the publisher's website.